Original Article
A novel mechanism driving poor-prognostic gastric cancer: overexpression of the transcription factor Krüppel-like factor 16 promotes growth and metastasis of gastric cancer through regulating the Notch pathway

Ding-Ping Sun[1,2], Yu-Feng Tian[1], Chih-Chan Lin[3], Shih-Ting Hung[3], Yih-Huei Uen[4,5,6], You-Cheng Hseu[7,8,9], Chia-Lin Chou[1], Li-Chin Cheng[1], Wen-Ching Wang[1], Yi-Yu Kuang[3], Chia-Lang Fang[10,11], Kai-Yuan Lin[3,12]

[1]Department of Surgery, Chi Mei Medical Center, Tainan 71004, Taiwan; [2]Department of Food Science and Technology, Chia Nan University of Pharmacy and Science, Tainan 71710, Taiwan; [3]Department of Medical Research, Chi Mei Medical Center, Tainan 71004, Taiwan; [4]Department of Surgery, Asia University Hospital, Taichung 41354, Taiwan; [5]Department of Biotechnology, Asia University, Taichung 41354, Taiwan; [6]Department of Surgery, Tainan Municipal An-Nan Hospital, Tainan 70965, Taiwan; [7]Department of Cosmeceutics, China Medical University, Taichung 40402, Taiwan; [8]Department of Health and Nutrition Biotechnology, Asia University, Taichung 41354, Taiwan; [9]Chinese Medicine Research Center, China Medical University, Taichung 40402, Taiwan; [10]Department of Pathology, School of Medicine, College of Medicine, Taipei Medical University, Taipei 11031, Taiwan; [11]Department of Pathology, Taipei Medical University Hospital, Taipei Medical University, Taipei 11031, Taiwan; [12]Department of Biotechnology, Chia Nan University of Pharmacy and Science, Tainan 71710, Taiwan

Abstract: Gastric cancer (GC) is one of the most common malignant tumors worldwide and has high rates of morbidity and mortality. This study investigated the role of Krüppel-like factor 16 (KLF16) in GC. Real-time polymerase chain reaction, Western blotting, and immunohistochemistry were used to examine the expression of KLF16 in gastric cells and tissues. Gene overexpression and silencing were applied to study the involvement of KLF16 in GC cell growth and metastasis along with its underlying mechanism. The results indicate that KLF16 overexpression is significantly associated with nodal status, distant metastasis, staging, degree of differentiation, vascular invasion, and patient survival. Multivariate Cox proportional hazards regression model analysis revealed that the overexpression of KLF16 is an independent prognostic biomarker of GC. The in vitro study revealed that up-regulated KLF16 accelerates cell growth and metastasis, whereas the inhibition of KLF16 suppresses these cellular activities. The results of an animal study also indicated that the overexpression and silencing of KLF16 accelerate and repress xenograft proliferation and metastasis. Further studies of affected cell growth and metastasis revealed that KLF16 modulates the cell cycle and epithelial-mesenchymal transition through transcriptional regulation of microfibrillar-associated protein 5. Collectively, these results reveal that KLF16 overexpression is a potential prognostic biomarker and therapeutic target for the treatment of GC.

Keywords: Gastric cancer, KLF16, prognosis, MFAP5, Notch pathway

Introduction

Gastric cancer (GC) remains a prevalent cancer worldwide [1]. Because the underlying pathogenic mechanisms of GC remain illusive, and few targeted drugs have been developed, the treatment of patients with GC remains an extremely challenging task in clinical practice [2, 3]. Technical advances facilitate the identification of aberrantly expressed molecules as novel biomarkers [4-9].

Krüppel-like factors (KLFs) are transcription factors that control essential cellular events [10]. Furthermore, prominent oncogenic functions are defined for various KLFs [10-13]. The function of KLF16 in cancer currently remains predominantly unclear and controversial. The facilitation of cell proliferation through the silencing of KLF16 in glioma cells suggests that KLF16 is a tumor suppressor [14]. By contrast, a study conducted in GC suggested an oncogenic role of KLF16 [15]. More studies are

required to understand the function of KLF16 in cancer. Research related to the prognostic value of KLFs is limited [16-18]. Marrero-Rodríguez and his colleagues demonstrated that KLF5 mRNA overexpression represented a prognostic marker for cervical cancer [19]. Only one study recognized the prognostic significance of KLF16 in human cancers, using univariate analysis to show that the overexpression of KLF16 could serve as a predictor of poor survival among patients with GC [15].

Numerous cellular functions associated with tumorigenesis are modulated by Notch signaling, including apoptosis, cell proliferation and epithelial-mesenchymal transition (EMT) [20]. The Notch intracellular domain (NICD) and pre-senilin-1, the catalytic subunit of γ-secretase, mediate Notch signaling [21]. Microfibrillar-associated protein 5 (MFAP5) was found to be a Notch ligand that could activate the Notch pathway [22]. The up-regulation of MFAP5 has already been noted in several cancers, including breast cancer and cervical cancer [23, 24]. So far, the MFAP5 level in GC remains unclear and requires further examination. Establishing whether MFAP5 is a target gene of KLF16 in GC cells would also improve understanding of how the overexpression of KLF16 can promote GC carcinogenesis.

In this paper, we examine the KLF16 level in GC and analyze the correlations of KLF16 with clinicopathologic features and patient survival. We also study the effect of KLF16 manipulation on cell growth, cell cycle progression, cell migration and invasion, xenograft proliferation and peritoneal metastasis. The mechanism of tumorigenicity involving KLF16 is also investigated.

Materials and methods

Cell culture

The human normal gastric cell line Hs738.St/Int (provided by the American Type Culture Collection; Manassas, VA, USA) was cultured in DMEM. GC cell line AGS (provided by the Bioresource Collection and Research Center; Hsinchu, Taiwan) was grown in F-12K. GC cell lines, including NCI-N87, TMC-1, TSGH 9201 (provided by the Bioresource Collection and Research Center; Hsinchu, Taiwan), SK-GT-2 (provided by the European Collection of Cell Cultures; Salisbury, UK), and 23132/87 (provided by Creative Bioarray; Shirley, NY, USA), were maintained in RPMI-1640. GC cell line HGC-27 (provided by the European Collection of Cell Cultures; Salisbury, UK) was cultured in MEM. All media were supplemented with 10% fetal bovine serum and antibiotics. All cell lines were authenticated by cell providers. We also checked the ICLAC database to ensure that all cell lines were not misidentified.

Patients and tissue specimens

For this study, gastric tissue specimens were collected from 142 patients with GC who underwent surgical resection at Taipei Medical University Wan Fang Hospital between 1998 and 2011 (**Table 1**). A retrospective power analysis was conducted to determine the association of KLF16 level with disease-free and overall survival. This analysis showed that the study had approximately 99% power to detect a significant difference (effect size = 0.54) from the observed data, assuming a significance level of α = 5%. This study was conducted in accordance with the Helsinki declaration and was approved by the Institutional Review Board of Taipei Medical University Wan Fang Hospital (Approval No. 99049), and each patient provided written informed consent in advance.

Antibodies

Antibodies against KLF16 and Ki67 were purchased from Novus (Centennial, CO, USA). Those against cyclin B, cyclin E, CDK1, CDK2, E-cadherin, and Slug were obtained from Arigo (Hsinchu, Taiwan). The antibodies against β-catenin, AKT and phosphor-AKT were purchased from Thermo (Waltham, MA, USA), and that against N-cadherin was purchased from BD (San Jose, CA, USA). The antibody against MFAP5 was obtained from LifeSpan (Seattle, WA, USA), those against PI3K, NICD and presenilin-1 were purchased from Cell Signaling (Danvers, MA, USA), and that against β-actin was purchased from Sigma (St. Louis, MO, USA).

RNA extraction

Total RNA from gastric cells was extracted using TRIzol reagent according to the manufacturer's protocol (Sigma). After chloroform separation, the aqueous phase was collected, and

Table 1. Demographic data and survival in different stages of GC according to the AJCC classification

	Stage I (n = 25)	Stage II (n = 37)	Stage III (n = 66)	Stage IV (n = 14)	Total (n = 142)
Gender					
Male	15	25	46	10	96
Female	10	12	20	4	46
Age (years)*	67.6 (12.7)	75.2 (10.3)	69.4 (13.3)	56.8 (14.8)	69.4 (13.5)
Follow-up period (months)*	44.5 (32.7)	31.5 (21.7)	27.1 (27.6)	13.3 (9.7)	29.9 (27.0)
Survival					
Yes	16	18	14	2	50
No	9	19	52	12	92

*Age and follow-up period are mean (SD).

RNA was precipitated by adding ice-cold isopropanol. After washing once with 75% ethanol, the pellets were air-dried to determine the RNA concentrations.

Quantitative polymerase chain reaction analysis

cDNA was synthesized from total RNA using a QuantiTect Reverse Transcription Kit (Qiagen, Valencia, CA, USA) following the instructions of the manufacturer. Total RNA was mixed with Genomic DNA Wipeout Buffer and incubated at 42°C for 2 minutes. Quantiscript RT Buffer, RT Primer Mix, and Quantiscript Reverse Transcriptase were added and incubated at 42°C for an additional 30 minutes. Primers for KLF16 and GAPDH, which was used as an internal control, and quantitative polymerase chain reaction master mix were purchased from Sigma. The expression levels of the target genes were measured using quantitative PCR in an Illumina Eco Quantitative PCR System (Illumina, San Diego, CA, USA). The threshold cycle (C_t) is the fractional cycle number at which the fluorescence generated by cleavage of the probe exceeds a fixed level above the baseline. For a chosen threshold, a smaller starting copy number results in a higher C_t value. The level of KLF16 mRNA in cells was standardized against the amount of GAPDH mRNA and was expressed as ΔC_{tumor} or $\Delta C_{non-tumor} = C_{t\,(KLF16)} - C_{t\,(GAPDH)}$.

RNA library preparation

Library preparation was performed with the NEBNext® Ultra™ Directional RNA Library Prep Kit for Illumina (NEW ENGLAND BioLabs, Cat.: #E7420). In brief, RNA was fragmented via heat and divalent metal cation method after poly-A

selected by NEBNext® Poly(A) mRNA Magnetic Isolation Module Kit (NEW ENGLAND BioLabs). Then the fragmented RNA was synthesized first strand cDNA by adding random primers to priming first. Then it proceeded to second strand (double-stranded) cDNA synthesis. The end repaired double-stranded cDNA library was ligated to the adaptors with the cut site of the USER enzyme. The library is then ready for amplification and size-selection by Purification Module with Agencourt AMPure XP Beads (Beckman coulter, Cat.: #A63881). The qualified libraries were analyzed by FRAGMENT ANALYZER™ Automated CE System (Advanced Analytical Technologies, Inc) and quantified by Qubit Fluorometer (Thermo). The libraries were sequenced with Illumina sequencing platform following the manufacturer's instruction.

Bioinformatics analysis

This pipeline was developed under Linux CentOS 6.6 environment. First, the reads shorter than 25 bps generally with low quality scores were also removed from the set. Second, the reads belong to rRNA were identified. After completing above preprocessing steps, the sequencing quality report was produced by using FastQC (http://www.bioinformatics.babraham.ac.uk/projects/fastqc). The subsequent sequence reads were aligned onto the reference sequence of the human genome using the TopHat2 splice-junction mapper and calculated expression value (Fragments Per Kilobase of exon per Million fragments mapped, FPKM = total fragments/mapped reads (M)* exon length (KB)) of each gene at either gene or isoform level. For differential expression analysis, we used Cuffdiff, an algorithm that robustly

estimates expression at transcript-level resolution and controls for variability evident across replicate (if present) libraries to identify differential expressed genes between scrambled and KLF16-knockdown HGC-27 cells.

Protein extraction and Western blotting

Total cell and tissue lysates were extracted with RIPA Buffer (Thermo). Denatured protein samples were subjected to 10% SDS-PAGE and transferred to nitrocellulose membranes. Blocked blots were incubated at 4°C overnight with primary antibodies. β-Actin was used as an internal control for equal protein loading. After incubation with secondary antibodies conjugated with peroxidase (Sigma), enhanced chemiluminescence reagents (Thermo) were used to visualize the targeted proteins. Image processing was performed using GeneTools software (Syngene, Cambridge, UK).

Immunohistochemistry

Paraffin-embedded sections were stained with primary antibodies at 4°C overnight. A standard peroxidase-conjugated streptavidin-biotin method was used to detect the immunoreactivity (Dako REAL EnVision Detection System; Dako, Carpinteria, CA, USA). Human small intestine was used as a positive control for KLF16. The negative control consisted of the omission of the primary antibody and incubation with 1× phosphate buffer saline (Corning). Images were acquired with BX51 microscope (Olympus, Tokyo, Japan). KLF16 immunoreactivity was assessed semiquantitatively and scored as follows: 0, no staining; 1, weak and focal staining in < 25% of the tissue; 2, moderate staining in 25%-50% of the tissue; and 3, strong staining in > 50% of the tissue. Sections with a score of 0 or 1 exhibited low expression of KLF16, and those with a score of 2 or 3 were defined as exhibiting high expression or overexpression of KLF16. Clinical data collection and immunohistochemical analysis were independently performed in an investigator-blinded study.

shRNA treatment

For shRNA treatment, HGC-27 cells were infected with lentiviral vectors (two KLF16-shRNA constructs, clone IDs: TRCN0000020004, TRCN0000020007, and one control, clone ID:

pLKO_TRC025, purchased from the National RNAi Core Facility, Taipei, Taiwan) and stable clones resistant to puromycin (Thermo) were selected. KLF16-overexpressing AGS cells were infected with lentiviral vectors (two MFAP5-shRNA constructs, clone IDs: TRCN0000152-652, TRCN0000153916, and one control, clone ID: pLKO_TRC025) and stable clones resistant to puromycin were selected. Western blotting was performed to evaluate the effects of shRNA treatment.

Transfection

AGS cells were transfected with Human KLF16 cDNA open reading frame and empty vectors (OriGene, Rockville, MD, USA) and stable clones resistant to G418 (Sigma) were selected. Western blotting was performed to evaluate the efficiency of transfection.

Colony formation assay

Five hundred cells were seeded into 6-well plates and cultured for 12 days. Individual colonies (> 50 cells/colony) were fixed, stained using a solution of 1% crystal violet in methanol, and counted. The plates were scanned with Scanjet 2200c scanner (HP, Palo Alto, CA, USA). After scanning, methanol was added, and the plates were shaken at room temperature to solubilize the crystal violet. The optical density (OD540) was measured to quantify the number of colony formed. The assay was conducted three 3 times, and the results were presented as the mean ± SD.

Cell cycle analysis

The cellular DNA content was determined by cell cycle analysis of propidium iodide-labeled cells, as described in our previous study [25].

Wound-healing assay

For the wound-healing assay, cells (5×10^5) were seeded into a 12-well culture dish and grown to a nearly confluent monolayer. The monolayers were carefully scratched using a 200 μL pipette tip. Cellular debris was removed by washing with 1× phosphate buffer saline, and the cells were then incubated for 18 hours. The cultures were photographed (100× magnification, with Leica DMIRB microscope, Leica, Wetzlar, Germany) at 0 and 18 hours to monitor the

migration of cells to the wounded area, and the number of migrated cells was quantified using Image J software. The percentage of cell migration was calculated by defining the number of migrated wild type cells as 100%. All experiments were performed in triplicate, and the results were presented as the mean ± SD.

Cell invasion assay

The cell invasive capability was examined using a Cell Invasion Assay Kit (Merck Millipore, Darmstadt, Germany), following the manufacturer's instructions. Complete media were first added to 24-well plates. The cells ($2×10^5$) in serum-free media were added to ECMatrix-layered cell culture inserts (containing 8 μm pore size polycarbonate membranes) and cultured for 24 hours. Before staining, the cells on the upper surface were removed. Inserts were then dipped in the Staining Solution to stain invaded cells on the lower surface of the membranes. The cultures were photographed (100× magnification, with Leica DMIRB microscope), and the number of invaded cells was counted. The percentage of cell invasion was calculated by defining the number of invaded wild type cells as 100%. The assay was conducted 3 times independently, and the results were presented as the mean ± SD.

Luciferase assay

Cells were seeded in triplicate in 6-well plates and cultured for 24 hours. Dual reporter plasmid (containing MFAP5 promoter, uses secreted Gaussia luciferase as the promoter reporter and secreted alkaline phosphatase as the internal control for signal normalization) (GeneCopoeia, Rockville, MD) were transfected into the indicated cells using TurboFectin transfection reagent (Thermo) according to the manufacturer's recommendations. Culture media were collected to measure luciferase and alkaline phosphatase signals 36 hours after transfection using the Secrete-Pair Dual Luciferase Assay Kit (Genecopoeia) according to the manufacturer's protocol.

Animals

Male athymic 4-week-old BALB/c nude mice were obtained from the National Laboratory Animal Center, Taiwan. All experimental procedures involving animals were approved by the Chi Mei Medical Center Animal Ethics Research Board (Approval No. 103121520).

Tumor cell inoculation for xenograft proliferation

To investigate KLF16 overexpression, nude mice were divided into 2 groups (5 mice/group) for tumor cell inoculation. The control and KLF16-overexpressing AGS cells ($5×10^6$) were mixed with 200 μL of Matrix gel (Corning, New York, NY, USA) and injected subcutaneously into the right hind flank. The mice were sacrificed and photographed (with a CANON EOS 800D camera, CANON, Tokyo, Japan) 6 weeks after inoculation. The tumors were then removed and weighed. To investigate KLF16 knockdown, KLF16-knockdown and control HGC-27 cells were used for inoculation. The mice were sacrificed 6 weeks after inoculation.

Tumor cell inoculation for xenograft metastasis

The scrambled control and KLF16-knockdown HGC-27 cells were intraperitoneally injected into the mice ($1×10^7$ cells in 500 mL of 1× phosphate buffer saline, 5 mice/group). Mice were inspected every 2 days and killed 6 weeks after injection. Solid tumors were removed and examined.

Statistical analysis

The difference between KLF16 levels in tumor and nontumor tissues was analyzed using a paired *t* test. The differences in cell growth, migration, and invasion between control and KLF16-manipulated cells were examined using Student's *t* tests. The correlation between KLF16 level and clinicopathologic features was analyzed using the χ^2 test. Kaplan-Meier and log-rank tests were used to compare disease-free and overall survival and to create survival curves based on high and low KLF16 immunohistochemical scores. Multivariate survival analysis was performed for all features indicated to be significant in univariate survival analysis using the Cox proportional hazards model. All data were analyzed using SPSS version 24.0 (IBM, Armonk, NY, USA). All statistical tests were 2-sided, and $P < 0.05$ was considered significant.

Results

The KLF16 levels in GC

First, KLF16 mRNA and protein levels in 8 gastric cells were measured to clarify the involve-

Krüppel-like factor 16 is a prognostic biomarker for gastric cancer
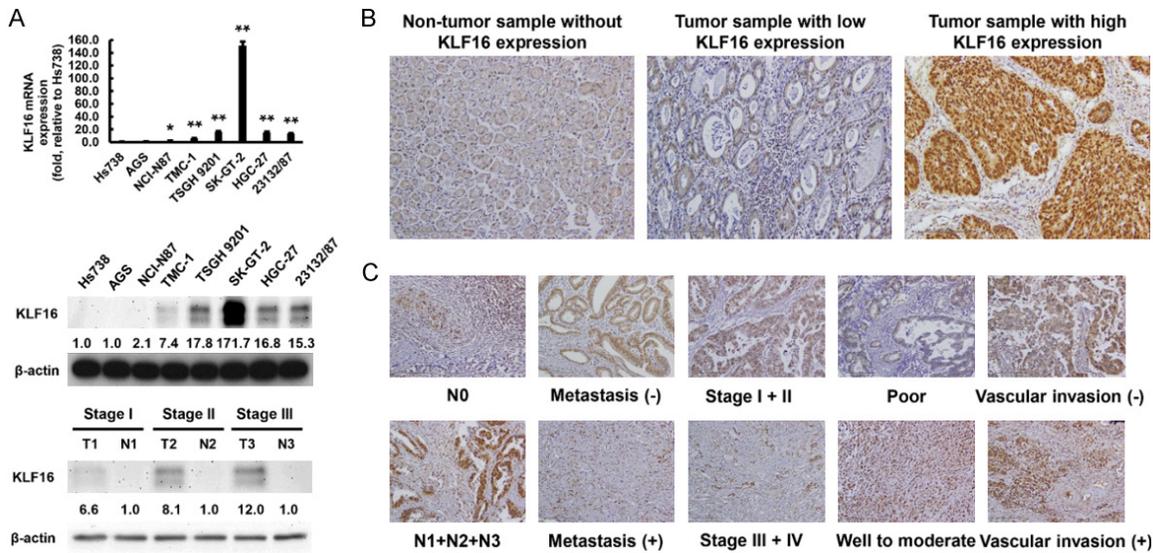
Figure 1. KLF16 expression in gastric cell lines and tissues. A. Endogenous KLF16 mRNA and protein expression were remarkably increased in GC cell lines and tissues. *denotes $P < 0.05$ compared with Hs738.St/Int. **denotes $P < 0.01$ compared with Hs738.St/Int cells. B. GC analyzed by immunohistochemistry with an antibody against KLF16. Left panel shows a non-tumor sample without KLF16 expression; middle panel shows a tumor sample with low KLF16 expression; right panel shows a tumor sample with high KLF16 expression. Magnification: 200×. C. The representative KLF16 staining for different clinicopathologic features. Magnification: 200×.

ment of KLF16 in the pathological process of GC. As shown in **Figure 1A**, KLF16 mRNA and protein levels were markedly higher in several GC cell lines (TMC-1, TSGH 9201, SK-GT-2, HGC-27 and 23132/87) than in Hs738.St/Int cells (quantification data are presented in Figure S1A). The KLF16 protein level in gastric tissues collected from a cohort of patients with GC was also measured and was found to be up-regulated compared with in nontumor tissues (representative photos are shown in **Figure 1B**). **Figure 1A** also reveals that KLF16 levels are higher in tumor tissues than in nontumor tissues (quantification data are presented in Figure S1B). As GC progresses, the level of KLF16 also increases. The results indicate that KLF16 level is increased in GC, especially in advanced-stage GC.

Associations of KLF16 expression with clinicopathologic features and the survival of patients with GC

We further studied the association between KLF16 expression and clinicopathologic features as well as the prognosis of patients with GC. **Table 2** reveals that KLF16 level was significantly associated with nodal status, distant metastasis, staging, degree of differentiation,

and vascular invasion. Representative photos for these clinicopathologic features are presented in **Figure 1C**.

Furthermore, we found that patients with GC whose KLF16 levels were high exhibited shorter disease-free and overall survival than did those whose KLF16 levels were low (**Figure 2A** and **2B**). The results of univariate analysis indicated that KLF16 overexpression, depth of invasion, nodal status, distant metastasis, staging, and vascular invasion are prognostic biomarkers. In a multivariate analysis, KLF16 and distant metastasis were prognostically independent (**Table 3**). These data suggest that KLF16 may be in involved in GC pathogenesis.

Effect of KLF16 manipulation on cell growth and cell cycle progression

The HGC-27 cell line was selected because of its abundance of KLF16 to clarify the function of KLF16 in GC cell growth. KLF16-knockdown efficiency was confirmed through Western blotting (**Figure 3A**) (quantification data are presented in Figure S2). **Figure 3B** reveals the colony-forming ability of HGC-27 to be inhibited by KLF16 silencing (quantification data are presented in Figure S3A).

2722

Am J Cancer Res 2021;11(6):2717-2735

Table 2. Clinical features of GC patients according to high or low KLF16 expression

Variable	n	KLF16 expression		P*
		Score = 0 or 1 (n = 58)	Score = 2 or 3 (n = 84)	
Age				0.5131
≥ 66	95	37	58	
< 66	47	21	26	
Gender				0.9386
Male	96	39	57	
Female	46	19	27	
Lauren classification				0.3008
Intestinal	101	44	57	
Diffuse	41	14	27	
Depth of invasion				0.3980
T1 + T2	34	16	18	
T3 + T4	108	42	66	
Nodal status				0.0004
N0	45	28	17	
N1 + N2 + N3	97	30	67	
Distant metastasis				0.0011
Absent	128	58	70	
Present	14	0	14	
Stage				0.0028
I + II	62	34	28	
III + IV	80	24	56	
Degree of differentiation				0.0033
Poor	60	16	44	
Well to moderate	82	42	40	
Vascular invasion				0.0185
Absent	41	32	18	
Present	101	35	66	

*All statistical tests were 2-sided. Significance level: $P < 0.05$.

Cell cycle progression was analyzed using flow cytometry, and the results indicated that KLF16 silencing impaired the G0/G1-S transition of cell cycle progression (**Figure 3C**).

The AGS cell line was also selected because of its low KLF16 level to further clarify the function of KLF16 in GC cell growth. KLF16 overexpression was confirmed through Western blotting (**Figure 3A**). **Figure 3B** reveals rev that more colonies were formed by KLF16-overexpressing AGS cells (quantification data are presented in Figure S3B).

The cell cycle is controlled by various cyclins and CDKs. Cyclin and CDK levels were measured to evaluate the underlying mechanism of G0/G1 arrest caused by KLF16 abrogation. **Figure 3D** shows that the levels of cyclin E and

CDK2, G1 phase regulators, were decreased in KLF16-knockdown HGC-27 cells. By contrast, the levels of cyclin B and CDK1, G2 phase regulators, were unchanged (**Figure 3D**) (quantification data are presented in Figure S4).

To assess the involvement of PI3K/AKT in KLF16-mediated cell growth and survival, we also investigated the effect of KLF16 silencing on the levels of PI3K and phosphor-AKT [26]. We found that PI3K and phospho-AKT levels were reduced in KLF16-silencing HGC-27 cells (Figure S5).

We measured the levels of various cyclins, CDKs, PI3K and phospho-AKT in KLF16-overexpressing AGS cells to validate the data of HGC-27 cells. **Figure 3D** shows that cyclin E and CDK2 levels were increased in KLF16-
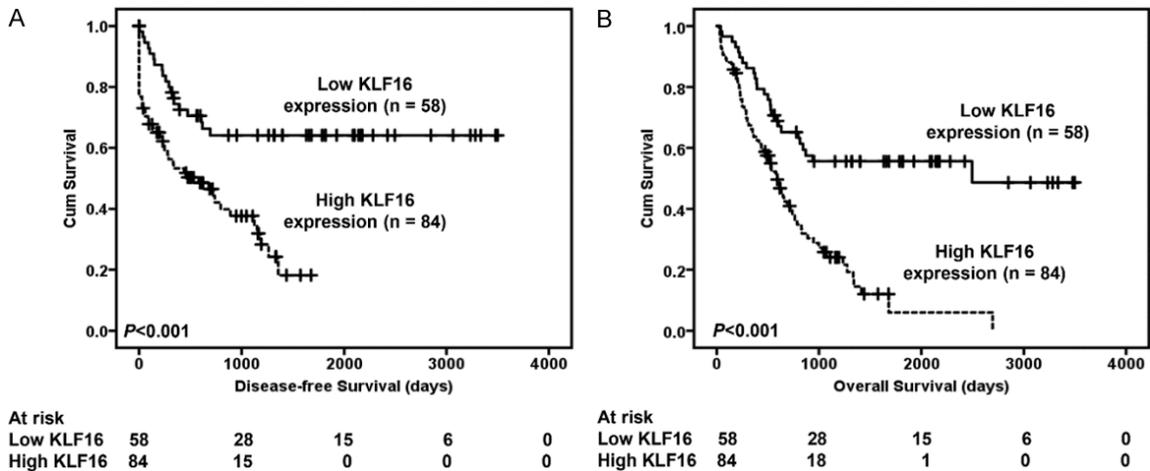
Figure 2. Survival analysis of GC patients stratified by KLF16 immunoreactivity. (A) shows the disease-free survival. Patients with high KLF16 expression had a 5-year disease-free survival rate of 18.2% compared with 64.1% for patients with low KLF16 expression. (B) shows the overall survival. Patients with high KLF16 expression had a 5-year disease-free survival rate of 6.0% compared with 55.6% for patients with low KLF16 expression. All statistical tests were 2-sided. Significance level: $P < 0.05$.

Table 3. Univariate and multivariate Cox regression analyses of prognostic biomarkers and survival in 142 GC patients

Variable	Univariate		Multivariate	
	hazard ratio (95% confidence interval)	P^*	hazard ratio (95% confidence interval)	P^*
KLF16	2.743 (1.597-4.709)	< 0.001	1.872 (1.048-3.342)	0.034
Low expression vs. High expression				
Age	1.394 (0.826-2.353)	0.213		
≥ 66 vs. < 66				
Gender	0.721 (0.424-1.226)	0.227		
Male vs. Female				
Lauren classification	1.194 (0.708-2014)	0.505		
Intestinal vs. Diffuse				
Depth of invasion	3.541 (1.617-7.755)	0.002	1.581 (0.634-3.937)	0.326
T1 + T2 vs. T3 + T4				
Nodal status	4.348 (2.211-8.552)	< 0.001	1.450 (0.526-3.995)	0.472
N0 vs. N1 + N2 + N3				
Distant metastasis	13.179 (5.387-32.239)	< 0.001	7.536 (3.000-18.928)	< 0.001
Absence vs. Presence				
Stage	4.464 (2.502-7.964)	< 0.001	2.012 (0.810-4.998)	0.132
I + II vs. III + IV				
Degree of differentiation	0.680 (0.421-1.098)	0.115		
Poor vs. Well to moderate				
Vascular invasion	2.872 (1.533-5.377)	0.001	1.308 (0.645-2.650)	0.457
Absent vs. Present				

*All statistical tests were 2-sided. Significance level: $P < 0.05$.

overexpressing AGS cells. However, the level of cyclin B remained unchanged (**Figure 3D**). In addition, the levels of PI3K and phospho-AKT were also increased (Figure S5). The data
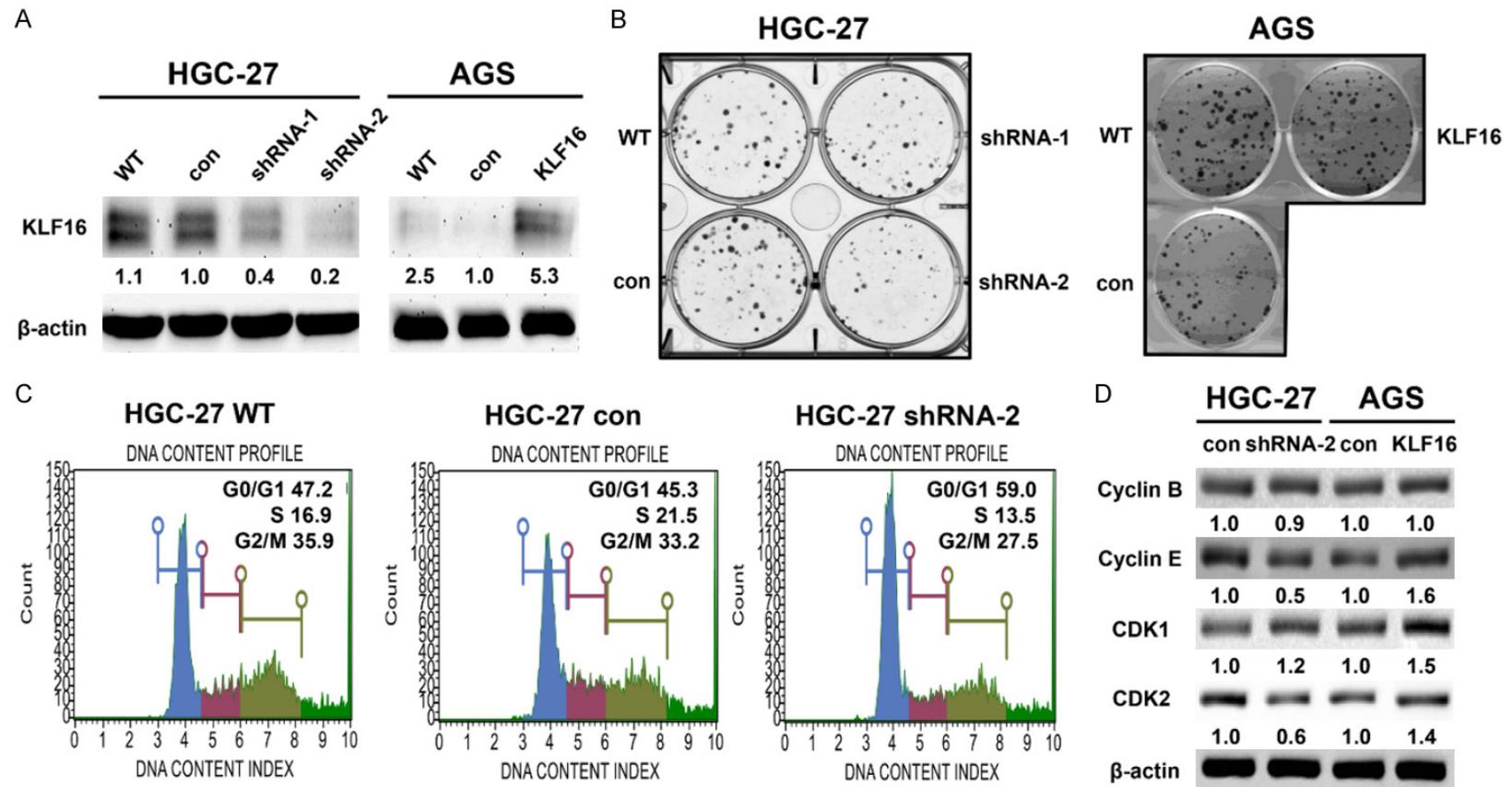
Figure 3. Verification of KLF16 manipulation in HGC-27 and AGS cells, and the effect of stable KLF16 manipulation on cell growth, cell cycle distribution, and the expression of cell cycle control molecules in the cells. A. The Western blotting results indicate KLF16 was efficiently knockdown by shRNA treatment and overexpressed by transfection. B. Stable KLF16 knockdown and overexpression resulted in markedly decreased and increased colony formation, respectively. C. Stable KLF16 knockdown resulted in a sustained accumulation of cells in the G0/G1 phase. Cellular distribution (as percentages) in different phases of the cell cycle (G0/G1, S, and G2/M) is presented as the mean of 3 independent experiments. D. Stable KLF16 knockdown and overexpression clearly decreased and increased the expression of cyclin E and CDK2, respectively. WT: non-transduced or non-transfected cells; con: scrambled control or control vector-transfected cells; shRNA: KLF16-knockdown cells; KLF16: KLF16-overexpressing cells.
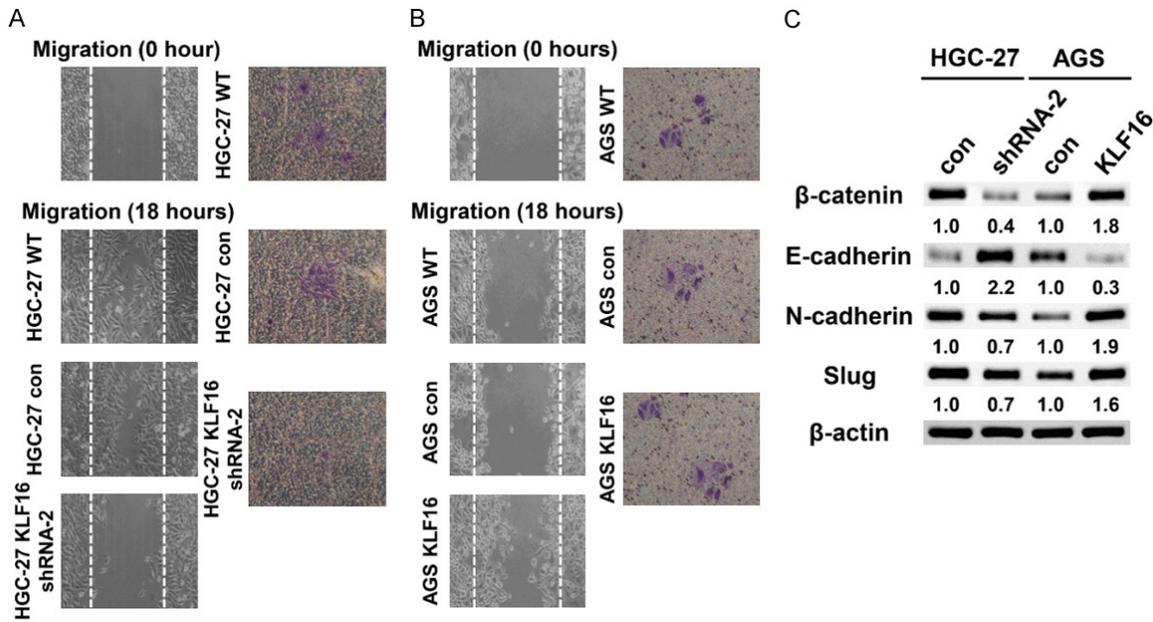
Figure 4. Effect of KLF16 manipulation in HGC-27 and AGS cells on cell spreading and the expression of EMT-related molecules. A. Stable KLF16 knockdown markedly decreased cell migration and invasion. B. Stable KLF16 overexpression obviously increased cell migration and invasion. C. Stable KLF16 manipulation resulted in the dysregulated expression of EMT-related molecules. WT: non-transduced or non-transfected cells; con: scrambled control or control vector-transfected cells; shRNA: KLF16-knockdown cells; KLF16: KLF16-overexpressing cells.

Table 4. Genes down-regulated in KLF16 knockdown HGC-27 cells

Gene ID	Log_2 (fold change)	P	Significant
FHL1	-4.2052	0.0003	yes
LY6G5C	-3.7204	0.0097	yes
KRT4	-3.3490	0.0085	yes
ACTA2	-3.2681	0.0001	yes
ACTG2	-3.2079	0.0015	yes
TINAGL1	-2.9013	0.0065	yes
MFAP5	-2.8964	0.0025	yes
HSD17B2	-2.8493	0.0003	yes
TNNC1	-2.7696	0.0009	yes
SRRM4	-2.6667	0.0011	yes
SAMD12	-2.6086	0.0005	yes
CAPN3	-2.5823	0.0035	yes
FOLR1	-2.5479	0.0001	yes
EGR1	-2.46811	0.0001	yes

reveal the function and mechanism of KLF16 in cell growth promotion.

Effect of KLF16 manipulation on cell migration and invasion

The associations between KLF16 level and nodal status, distant metastasis, and vascular invasion prompted us to study the effect of KLF16 manipulation on cell migration and inva-

sion. As indicated in **Figure 4A**, cell migration and invasion were suppressed in KLF16-knockdown HGC-27 cells (quantification data are shown in Figure S6A and S6B).

EMT, which confers metastatic properties on cancer cells, involves β-catenin, E-cadherin, N-cadherin and Slug. **Figure 4C** shows that KLF16 abrogation repressed β-catenin, N-cadherin and Slug expression. E-cadherin level was discovered to be increased after KLF16 knockdown.

To confirm the data of HGC-27 cells, cell migration and invasion assays were also performed for KLF16-overexpressing AGS cells. **Figure 4B** shows that cell migration and invasion were accelerated in KLF16 overexpression in AGS cells (quantification data are shown in Figure S6C and S6D). Moreover, KLF16 overexpression increased β-catenin, N-cadherin and Slug levels, and reduced E-cadherin level (**Figure 4C**) (quantification data are presented in Figure S4). These results demonstrate the function and mechanism of KLF16 in promoting cell migration and invasion.

Regulation of MFAP5 by KLF16

To further understand the underlying mechanism responsible for KLF16-regulated cell pro-
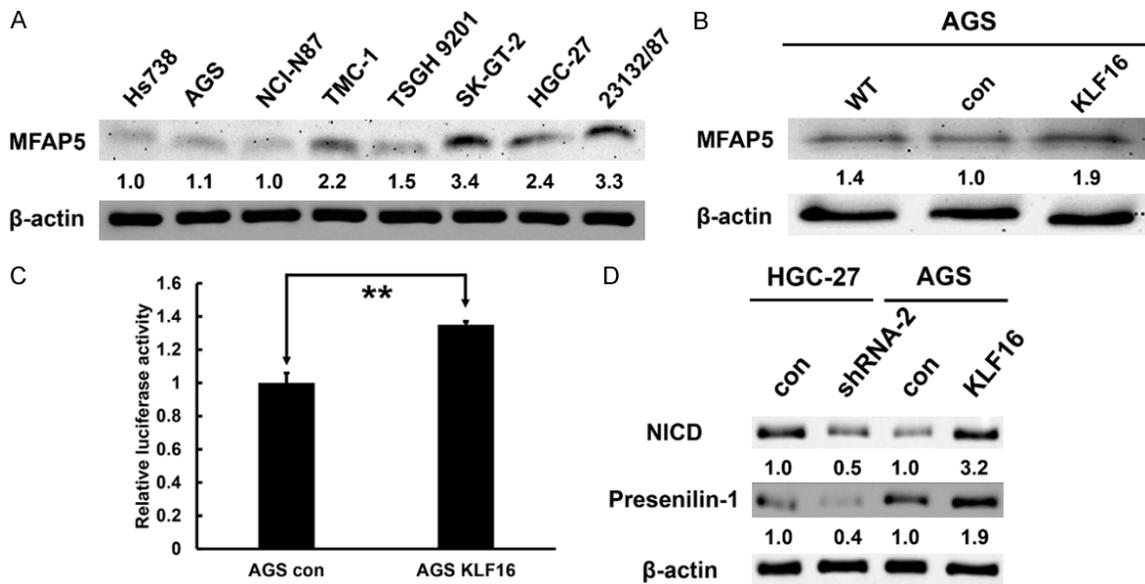
Figure 5. MFAP5, NICD and presenilin-1 expression in gastric cells and the relationship between MFAP5 and KLF16. A. MFAP5 protein expression was markedly increased in GC cells as compared with that in Hs738.St/Int cells. B. Stable KLF16 overexpression clearly increased the expression of MFAP5. C. There was a direct target relationship between MFAP5 and KLF16. **denotes $P < 0.01$ compared with the control. D. Stable KLF16 knockdown and overexpression resulted in markedly decreased and increased expression of NICD and presenilin-1, respectively. WT: non-transduced or non-transfected cells; con: scrambled control or control vector-transfected cells; shRNA: KLF16-knockdown cells; KLF16: KLF16-overexpressing cells.

liferation, migration, and invasion and to identify the direct targets of KLF16, next-generation sequencing was employed in KLF16-knockdown HGC-27 cells. **Table 4** lists down-regulated genes in KLF16-knockdown HGC-27 cells. The whole list of genes was shown in Table S1. Among the differentially expressed genes, MFAP5 attracted our attention and interest for its involvement in the Notch pathway. The MFAP5 level in 8 gastric cell lines was detected. **Figure 5A** indicates that the MFAP5 level was notably increased in TMC-1, SK-GT-2, HGC-27, and 23132/87 cells. Western blotting was also used to measure MFAP5 expression in KLF16-overexpressing AGS cells (quantification data are presented in Figure S7A). **Figure 5B** shows that MFAP5 was increased in KLF16-overexpressing AGS cells, suggesting a correlation between KLF16 and MFAP5 expression (quantification data are presented in Figure S7B). A luciferase assay was performed to further confirm the direct targeting relationship between KLF16 and the MFAP5 promoter. The results reveal that KLF16 overexpression significantly increase luciferase activity associated with the MFAP5 promoter (**Figure 5C**). These data reveal a direct targeting relationship

between KLF16 and the MFAP5 promoter. In addition to MFAP5, presenilin-1 and NICD expression were examined in KLF16-manipulated GC cells. **Figure 5D** indicates that the NICD and presenilin-1 levels were decreased in KLF16-knockdown HGC-27 cells but increased in KLF16-overexpressing AGS cells (quantification data are presented in Figure S8). The results further confirm that KLF16 exerts its oncogenic function through regulation of the Notch pathway.

Repression of cell growth and induction of cell cycle arrest in KLF16-overexpressing AGS cells through MFAP5 abrogation

To test whether KLF16 overexpression-promoted cell growth, migration and invasion can be reversed through knockdown of MFAP5, KLF16-overexpressing AGS cells were infected with MFAP5 shRNA lentiviruses (**Figure 6A**) (quantification data are presented in Figure S7C). **Figure 6B** shows that KLF16-overexpressing MFAP5-knockdown AGS cells formed fewer colonies.

Cell cycle progression was further analyzed, and the results indicated that MFAP5 knockdown interferes with G0/G1-S transition in
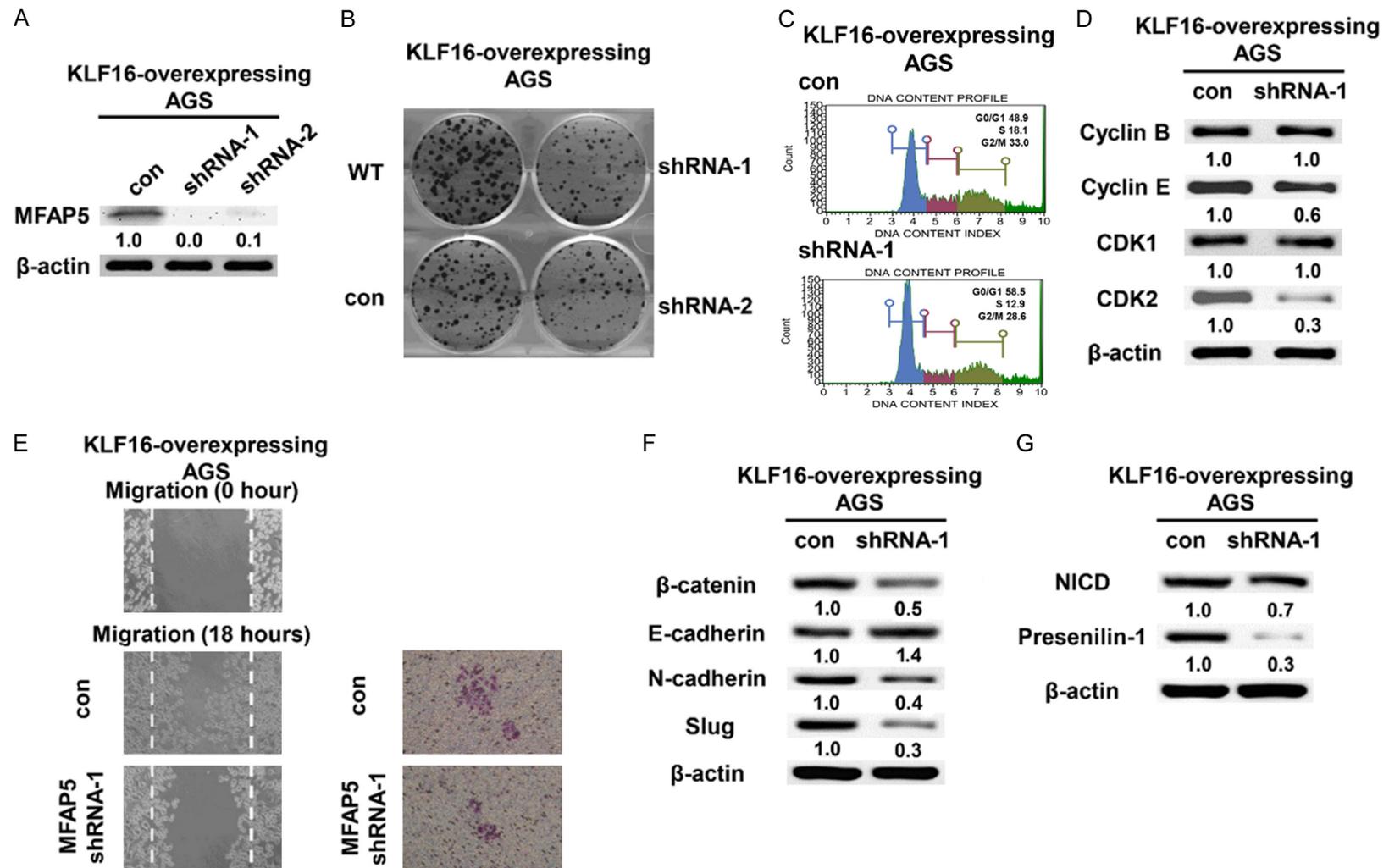
Figure 6. Effect of MFAP5 knockdown in KLF16-overexpressing AGS cells on cell growth, cell cycle distribution, cell spreading and the expression of cell cycle-, EMT- and Notch-related molecules. (A) The Western blotting results indicate MFAP5 was efficiently knockdown by shRNA treatment. con: scrambled control cells. (B) Stable MFAP5 knockdown obviously decreased colony formation. (C) Stable MFAP5 knockdown resulted in a sustained accumulation of cells in the G0/G1 phase. (D) Stable MFAP5 knockdown markedly decreased the expression of cyclin (E) and CDK2. Stable MFAP5 knockdown clearly decreased cell migration and invasion. (F) Stable MFAP5 knockdown resulted in the dysregulated expression of EMT-related molecules. (G) Stable MFAP5 knockdown markedly decreased the expression of NICD and presenilin-1. WT: non-transduced cells; con: scrambled control cells; shRNA: MFAP5 knockdown cells.

KLF16-overexpressing MFAP5-knockdown AGS cells (**Figure 6C**).

We next determine cyclin and CDK levels to explore the underlying mechanism of MFAP5 silencing-caused G0/G1 arrest. **Figure 6D** illustrates the decrease in cyclin E and CDK2 levels in KLF16-overexpressing MFAP5-knockdown AGS cells. By contrast, the levels of cyclin B and CDK1 were unchanged (**Figure 6D**) (quantification data are presented in Figure S9).

We also investigated the effect of MFAP5 knockdown on the levels of PI3K and phospho-AKT. PI3K and phospho-AKT levels were observed to be decreased in KLF16-overexpressing MFAP5-knockdown AGS cells (Figure S10). These data suggest that KLF16 overexpression-promoted cell growth can be suppressed through the knockdown of MFAP5.

The influence of MFAP5 knockdown on cell migration and invasion was also investigated. As indicated in **Figure 6E**, cell migration and invasion were suppressed in KLF16-overexpressing MFAP5-knockdown AGS cells.

The levels of EMT-related molecules were further detected, and the data indicated that MFAP5 knockdown reduced β-catenin, N-cadherin, and Slug levels (**Figure 6F**) (quantification data are presented in Figure S9). Up-regulated expression of E-cadherin was detected after MFAP5 knockdown. The data reveal that KLF16 overexpression-promoted migration and invasion can be repressed through MFAP5 knockdown.

Furthermore, as shown in **Figure 6G**, NICD and presenilin-1 expression was decreased in KLF16-overexpressing MFAP5-knockdown AGS cells (quantification data are presented in Figure S9). These results further confirm that KLF16 overexpression-activated Notch pathway can be suppressed through MFAP5 knockdown.

To rule out the possibility that KLF16 and MFAP5 can act at two parallel pathways to regulate cell proliferation, migration and invasion, we compared control AGS, MFAP5-knockdown AGS, KLF16-overexpressing AGS and KLF16 overexpressing, MFAP5-knockdown AGS. The results indicate that KLF16 overexpression promotes cell proliferation, migration and invasion

while knockdown of MFAP5 abolishes the effect of KLF16 overexpression on cell proliferation, migration and invasion (Figure S11).

Effect of KLF16 manipulation on xenograft proliferation and metastasis

The in vitro data suggest an oncogenic role of KLF16 in vivo. **Figure 7A** shows that 6 weeks after inoculation, the weight of scrambled control tumors was 2.8-fold higher than that of KLF16-knockdown tumors. Furthermore, the mitotic index, as indicated by Ki67 staining, was decreased in KLF16-knockdown tumors (Figure S12A).

To validate the data from KLF16-knockdown tumors, the same experiments were also performed for KLF16-overexpressing tumors. **Figure 7B** shows that the weight of KLF16-overexpressing tumors was 2.9-fold higher than that of vector control tumors. Moreover, the mitotic index was increased in KLF16-overexpressing tumors (Figure S12B). The results demonstrate the function of KLF16 in promoting tumor growth.

We subsequently studied the in vivo effect of KLF16 silencing on metastasis. Six weeks after the intraperitoneal injection, tumors in the mesentery and abdominal cavity were more numerous and larger in the control group than in the KLF16-knockdown group (**Figure 7C**). These data suggest that KLF16 has a function in the promotion of tumor metastasis.

*Reversal of KLF16-promoted GC tumor growth through MFAP5 silencing*

Finally, an animal study was conducted to validate the effects of MFAP5 knockdown on KLF16-promoted tumor growth. **Figure 7D** shows that the weight of KLF16-overexpressing MFAP5 scrambled control tumors was 5-fold higher than that of KLF16-overexpressing MFAP5-knockdown tumors. The data reveal that abrogating MFAP5 suppresses KLF-promoted tumor growth.

Our results suggest that KLF16 promotes proliferative and metastatic signals in GC cells through the Notch signaling pathway (**Figure 8**). Overexpressed KLF16 up-regulates MFAP5, which in turn activates the non-canonical Notch pathway. NICD, generated through Notch path-
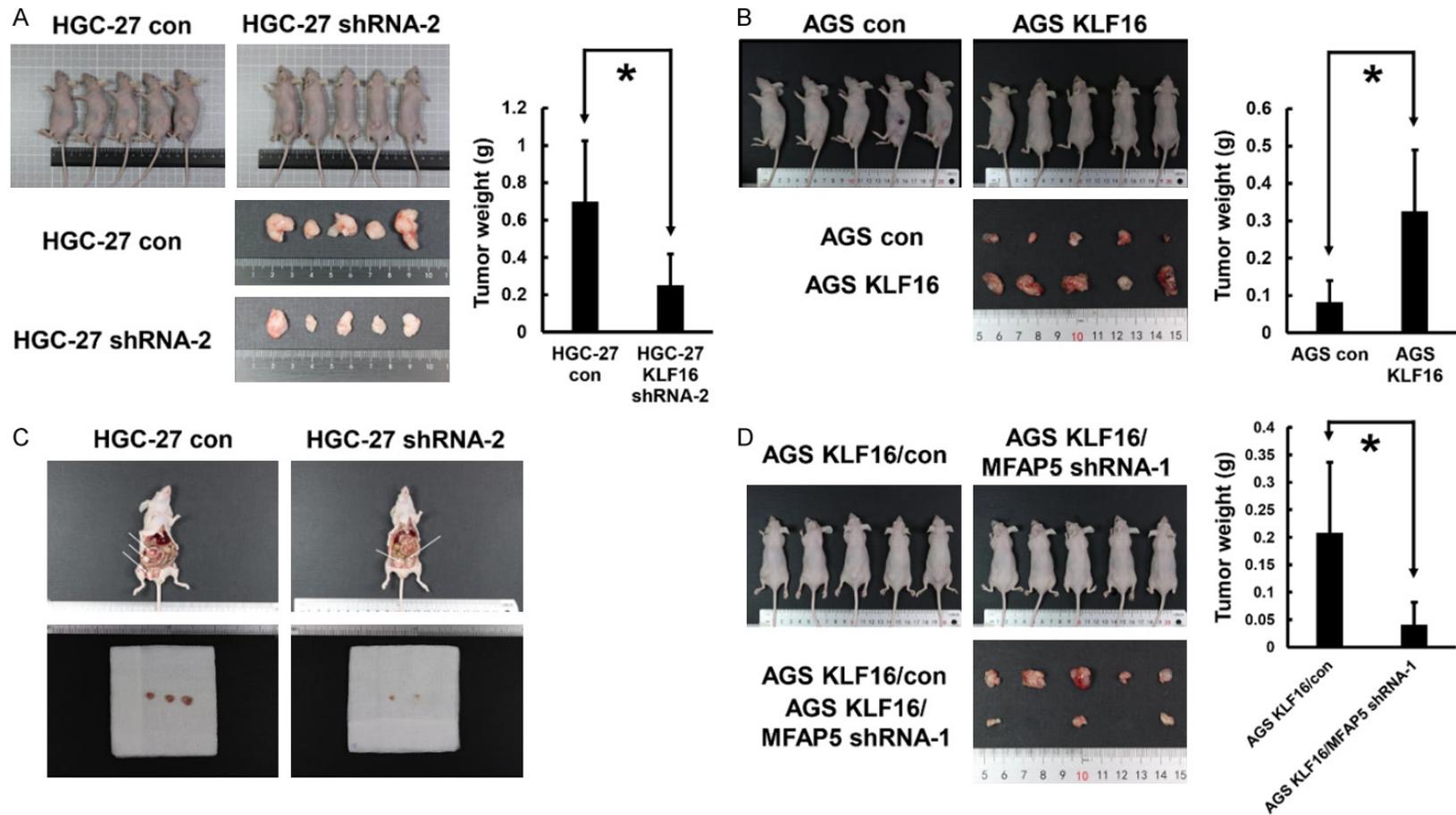
Figure 7. The effect of stable KLF16 manipulation in HGC-27 and AGS cells on in vivo tumor growth and metastasis in nude mice. A. Stable KLF16 knockdown resulted in the significant suppression of HGC-27 xenograft proliferation. The bar graph represents the results of the average tumor weight (presented as the mean ± SD, *P < 0.05). B. Stable KLF16 overexpression resulted in the significant enhancement of AGS xenograft proliferation. The bar graph represents the results of the average tumor weight (presented as the mean ± SD, *P < 0.05). C. Stable KLF16 knockdown resulted in the obvious suppression of HGC-27 xenograft metastasis. Peritoneal dissemination was recognized from the tumor nodules visualized in the abdominal cavity and mesenterium. The upper pictures show the peritoneal disseminations and the lower pictures show the dissected tumor nodules. Arrows in the pictures indicate the tumors developing peritoneal metastasis. D. Stable MFAP5 knockdown resulted in the significant suppression of KLF16-overexpressing AGS xenograft proliferation. The bar graph represents the results of the average tumor weight (presented as the mean ± SD, *P < 0.05). WT: non-transduced or non-transfected cells; con: scrambled control or control vector-transfected cells; shRNA: KLF16-knockdown cells; KLF16: KLF16-overexpressing cells.
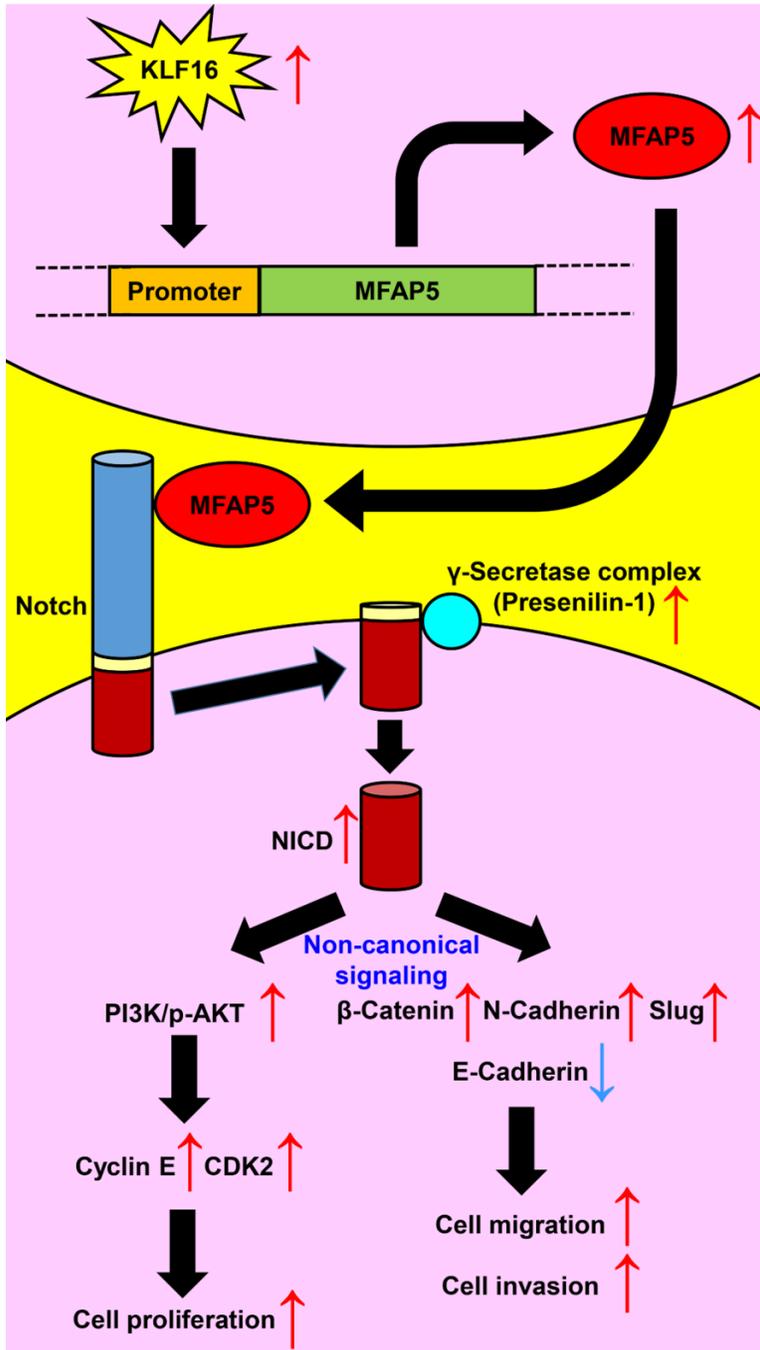
Figure 8. Model for the effects of KLF16 overexpression in GC. We propose a model in which KLF16 transcriptionally up-regulates MFAP5, which in turn, leads to an activation of the Notch pathway. Activation of Notch pathway, followed by augmentation of PI3K and phospho-AKT, increased cell cycle-related gene expression resulting in GC cell growth. Activation of the Notch pathway also increases EMT-related gene expression resulting in GC cell migration and invasion.

AKT levels. NICD also promotes cell spreading by increasing the number of EMT-related molecules. The inhibition of KLF16 can suppress KLF16-promoted cell proliferation, migration, and invasion; the inhibition of MFAP5 can compromise KLF16 overexpression-promoted cell proliferation, migration, and invasion.

Discussion

GC remains a prevalent cancer with high incidence and mortality rates, and it is a leading cause of cancer-related mortality worldwide [1]. Owing to distant metastasis, patients with advanced GC have fewer opportunities for surgery and shorter survival times than do patients with early GC [27, 28]. Many studies have demonstrated that GC emerges when molecular and genetic alterations accumulate in gastric epithelia [29]. The identification of underlying molecular mechanisms has benefitted GC prognosis and therapy, and the identification of molecular biomarkers associated with the prognostic and therapeutic targets of GC is urgently required.

Studies on the expression of KLF16 in cancers are scarce and inconsistent. Zhang et al. and Ma et al. have shown that KLF16 is overexpressed in glioblastoma and GC [15, 30]. By contrast, Chen et al. demonstrated that KLF16 expression is decreased in glioma [14]. In this study, we further established KLF16 levels in gastric tissues and cells. Similar to the findings of other studies, our findings indicated that KLF16 levels are increased in GC tissues and cells. Until now, the underly-

way activation, promotes cell proliferation by increasing the number of cell cycle-related molecules through up-regulation of PI3K/phospho-

ing mechanism of KLF16 up-regulation has remained mostly unknown. KLF16 was revealed to be overexpressed in glioblastoma and was targeted by miR-185-5p. Moreover, RNCR3 overexpression increased KLF16 levels through the inhibition of miR-185-5p expression [30]. Further studies are required to understand the underlying mechanism of KLF16 up-regulation.

Many members of the KLF family control cell proliferation. For example, KLF5 promotes cell proliferation by accelerating cells' passage through G1/S and G2/M phases of the cell cycle. Further investigation indicates that KLF5 targets cyclin D1, cyclin B1, and Cdc2 to promote cell cycle progression [31, 32]. Ectopic expression of KLF8, a mediator of focal adhesion kinase signaling, promotes cell cycle progression through activation of the cyclin D1 promoter [33]. KLF16 silencing increases p21 expression and reduces CDK4 expression in GC cell lines and, thereby markedly repressing cell proliferation. However, in glioma, KLF16 overexpression reduces cyclin D1 and cyclin E expressions, thereby reducing cell proliferation [14]. Research conducted by Fernandez-Zapico et al. also showed that KLF16 inhibits the ability of cancer cells to proliferate in vitro and in vivo [34]. In the present study, we investigated the function of KLF16 in cell growth through the manipulation of KLF16 expression. KLF16-overexpressing cells formed more colonies than did KLF16-knockdown cells, indicating that KLF16 can promote cell proliferation. KLF16-knockdown cells formed fewer colonies as a result of KLF16 knockdown-induced G0/G1 arrest. The Western blotting data of various cyclins and CDKs also indicated KLF16 knockdown-induced G0/G1 arrest. The levels of cyclin E and CDK2, but not those of cyclin B and CDK1, were observed to increase when KLF16 levels increased. In relation to regulation of the expression of cell cycle-related molecules by KLF16, Chen et al. found that in glioma, KLF16 overexpression reduces cyclin D1 and cyclin E expression through the direct targeting of mitochondrial transcription factor A and that the elevation of mitochondrial transcription factor A abrogated the effects of KLF16 overexpression on cyclin D1 and cyclin E expression [14]. Molecular studies conducted by Fernandez-Zapico et al. demonstrated that these effects by KLF16 are mediated by the silencing of cyclin A through binding to its promoter and subsequent cell cycle arrest in S phase [34]. In the

current study, when KLF16 was silenced, MFAP5 level was decreased; accordingly, cyclin E and CDK2 levels were down-regulated, causing G0/G1 cell cycle arrest. The Notch pathway is known to exhibit cross talk with other oncogenic pathways such as the PI3K/AKT pathway [35, 36]. We further found that when KLF16 was silenced, MFAP5 level decreased and the expression of PI3K and phosphorylation of AKT was inhibited. To the best of our knowledge, this is the first study to investigate the interaction between KLF16 and the Notch signaling pathway. Our conclusions are consistent with and extend those of another study also performed on patient with GC. Our data indicate that KLF16 can be a tumor suppressor gene or an oncogene, depending on the context.

Statistical analysis results revealed clinicopathologic correlations between KLF16 level and nodal status, distant metastasis, and vascular invasion and prompted us to study the roles of KLF16 in cell migration, invasion, and EMT. A review article published by Tetreault et al. stated that KLF5 can inhibit EMT in breast cancer cells through the up-regulation of E-cadherin, can reverse EMT in hepatocellular carcinoma cells through the repression of Slug, and undergoes down-regulation by Snail in colon cancer cells [11, 12, 37, 38]. KLF4 is another negative regulator of EMT and metastasis through the regulation of EMT-related genes such as E-cadherin and vimentin [39]. By contrast, KLF8 enhances breast cancer cell invasion and metastasis through the transcriptional suppression of E-cadherin and transactivating matrix metalloproteinase 9 [40, 41]. The roles of KLF16 in cell migration, invasion, and EMT remain unknown. This study found that KLF16 levels in GC cells are positively correlated with β-catenin, N-cadherin, and Slug levels and negatively correlated with E-cadherin level. Furthermore, the effects of KLF16 manipulation on cell migration and invasion were examined. The results suggest that KLF16 could increase the expressions of EMT-related molecules, followed by its facilitation of cell migration and invasion. This explains why the up-regulation of KLF16 is associated with nodal status, distant metastasis and vascular invasion. This is the first study is to investigate the KLF16/Notch/EMT axis.

No accurate biomarkers are currently known for the early diagnosis and prognosis of GC.

Most patients are diagnosed at advanced stages. Owing to the unsatisfactory prognosis for patients with GC, the key molecular mechanism of GC development must be identified to improve early diagnosis and personal treatment strategies for the disease [42]. Some research has studied the prognostic effects of KLFs on GC: Wang and his colleagues demonstrated that KLF2 level was decreased in GC. Moreover, down-regulated KLF2 expression in GC was closely correlated with patients' survival [43]. Mao et al. showed that KLF8 expression was significantly increased in GC tissues compared with adjacent normal tissues, and high KLF8 expression was correlated with inferior prognosis [44]. The current study identified a correlation between KLF16 up-regulation and poor patient survival and is the first study to recognize the possibility of KLF16 as a prognostic biomarker for GC. The current data also revealed that in patients with advanced GC, KLF16 is correlated with poor disease-free survival. Hence, patients with advanced GC should be followed up intensively.

Collectively, KLF16 promotes the tumorigenesis of GC, which is related to the activation of the Notch pathway, leading to significantly poor prognoses in patients with GC. Our findings also suggest that therapeutic strategies targeting KLF16 may provide effective treatments for GC.

Disclosure of conflict of interest

None.

Address correspondence to: Chia-Lang Fang, Department of Pathology, School of Medicine, College of Medicine, Taipei Medical University, Taipei 11031, Taiwan. E-mail: ccllfang@tmu.edu.tw; Kai-Yuan Lin, Department of Medical Research, Chi Mei Medical Center, Tainan 71004, Taiwan. E-mail: d970712@mail.chimei.org.tw

References

[1] Bray F, Ferlay J, Soerjomataram I, Siegel RL, Torre LA and Jemal A. Global cancer statistics 2018: GLOBOCAN estimates of incidence and mortality worldwide for 36 cancers in 185 countries. CA Cancer J Clin 2018; 68: 394-424.
[2] Thrift AP and El-Serag HB. Burden of gastric cancer. Clin Gastroenterol Hepatol 2020; 18: 534-542.
[3] Sun W and Yan L. Gastric cancer: current and evolving treatment landscape. Chin J Cancer 2016; 35: 83.
[4] Jin ZL, Jiang WH and Wang LW. Biomarkers for gastric cancer: progression in early diagnosis and prognosis. Oncol Lett 2015; 9: 1502-1508.
[5] Uen YH, Fang CL, Lin CC, Hseu YC, Hung ST, Sun DP and Lin KY. Ceramide synthase 6 predicts the prognosis of human gastric cancer: it functions as an oncoprotein by dysregulating the SOCS2/JAK2/STAT3 pathway. Mol Carcinog 2018; 57: 1675-1689.
[6] Fang CL, Lin CC, Chen HK, Hseu YC, Hung ST, Sun DP, Uen YH and Lin KY. Ubiquitin-specific protease 3 overexpression promotes gastric carcinogenesis and is predictive of poor patient prognosis. Cancer Sci 2018; 109: 3438-3449.
[7] Sun DP, Liew PL, Lin CC, Hung ST, Chen TC, Fang CL and Lin KY. Clinicopathologic and prognostic significance of thymopoietin-α overexpression in gastric cancer. J Cancer 2019; 10: 5099-5107.
[8] Zhang M, Dong BB, Lu M, Zheng MJ, Chen H, Ding JZ, Xu AM and Xu YH. miR-429 functions as a tumor suppressor by targeting FSCN1 in gastric cancer cells. Onco Targets Ther 2016; 9: 1123-1133.
[9] Zheng H, Zhang F, Lin X, Huang C, Zhang Y, Li Y, Lin J, Chen W and Lin X. MicroRNA-1225-5p inhibits proliferation and metastasis of gastric carcinoma through repressing insulin receptor substrate-1 and activation of β-catenin signaling. Oncotarget 2016; 7: 4647-4663.
[10] McConnell BB and Yang VW. Mammalian Kruppel-like factors in health and diseases. Physiol Rev 2010; 90: 1337-1381.
[11] Lin ZS, Chu HC, Yen YC, Lewis BC and Chen YW. Kruppel-like factor 4, a tumor suppressor in hepatocellular carcinoma cells reverts epithelial mesenchymal transition by suppressing slug expression. PLoS One 2012; 7: e43593.
[12] Yori JL, Johnson E, Zhou G, Jain MK and Keri RA. Kruppel-like factor 4 inhibits epithelial-to mesenchymal transition through regulation of E cadherin gene expression. J Biol Chem 2010; 285: 16854-16863.

[13] Nakamura Y, Migita T, Hosoda F, Okada N, Gotoh M, Arai Y, Fukushima M, Ohki M, Miyata S, Takeuchi K, Imoto I, Katai H, Yamaguchi T, Inazawa J, Hirohashi S, Ishikawa Y and Shibata T. Kruppel-like factor 12 plays a significant role in poorly differentiated gastric cancer progression. Int J Cancer 2009; 125: 1859-1867.

[14] Chen X, Li S, Ke Y, Wu S, Huang T, Hu W, Fu H and Guo X. KLF16 suppresses human glioma cell proliferation and tumourigenicity by targeting TFAM. Artif Cells Nanomed Biotechnol 2018; 46: 608-615.

[15] Ma P, Sun CQ, Wang YF, Pan YT, Chen QN, Liu WT, Liu J, Zhao CH, Shu YQ and Li W. KLF16 promotes proliferation in gastric cancer cells via regulating p21 and CDK4. Am J Transl Res 2017; 9: 3027-3036.

[16] Narla G, DiFeo A, Fernandez Y, Dhanasekaran S, Huang F, Sangodkar J, Hod E, Leake D, Friedman SL, Hall SJ, Chinnaiyan AM, Gerald WL, Rubin MA and Martignetti JA. KLF6-SV1 overexpression accelerates human and mouse prostate cancer progression and metastasis. J Clin Invest 2008; 118: 2711-2721.

[17] Humbert M, Halter V, Shan D, Laedrach J, Leibundgut EO, Baerlocher GM, Tobler A, Fey MF and Tschan MP. Deregulated expression of Kruppel-like factors in acute myeloid leukemia. Leuk Res 2011; 35: 909-913.

[18] Wei Y, Chen G, You L and Zhao Y. Krüpel-like factor 8 is a potential prognostic factor for pancreatic cancer. Chin Med J 2014; 127: 856-859.

[19] Marrero-Rodríguez D, Taniguchi-Ponciano K, Jimenez-Vega F, Romero-Morelos P, Mendoza-Rodríguez M, Mantilla A, Rodriguez-Esquivel M, Hernandez D, Hernandez A, Gomez-Gutierrez G, Muñoz-Hernandez N, la Cruz HA, Vargas-Requena C, Díaz-Hernández C, Serna-Reyna L, Meraz-Rios M, Bandala C, Ortiz-Leon J and Salcedo M. Krüppel-like factor 5 as potential molecular marker in cervical cancer and the KLF family profile expression. Tumour Biol 2014; 35: 11399-11407.

[20] Capaccione KM and Pine SR. The Notch signaling pathway as a mediator of tumor survival. Carcinogenesis 2013; 34: 1420-1430.

[21] Shih IM and Wang TL. Notch Signaling, γ-secretase inhibitors, and cancer therapy. Cancer Res 2007; 67: 1879-1882.

[22] Miyamoto A, Lau R, Hein PW, Shopley JM and Weinmaster G. Microfibrillar proteins MAGP-1 and MAGP-2 induce Notch1 extracellular domain dissociation and receptor activation. J Biol Chem 2006; 281: 10089-10097.

[23] Wu Y, Wu P, Zhang Q, Chen W, Liu X and Zheng W. MFAP5 promotes basal-like breast cancer progression by activating the EMT program. Cell Biosci 2019; 9: 24.

[24] Li Q, Zhang Y and Jiang Q. MFAP5 suppression inhibits migration/invasion, regulates cell cycle and induces apoptosis via promoting ROS production in cervical cancer. Biochem Biophys Res Commun 2018; 507: 51-58.

[25] Hseu YC, Cho HJ, Thiyagarajan V, Gowrisankar YV, Chen XZ, Lin KY, Huang HC and Yang HL. Kalantuboside B induced apoptosis and cytoprotective autophagy in A2058 human melanoma cells: an in vitro and in vivo study. Free Radic Biol Med 2019; 143: 397-411.

[26] Yu JS and Cui W. Proliferation, survival and metabolism: the role of PI3K/AKT/mTOR signaling in pluripotency and cell fate determination. Development 2016; 143: 3050-3060.

[27] Orditura M, Galizia G, Sforza V, Gambardella V, Fabozzi A, Laterza MM, Andreozzi F, Ventriglia J, Savastano B, Mabilia A, Lieto E, Ciardiello F and De Vita F. Treatment of gastric cancer. World J Gastroenterol 2014; 20: 1635-1649.

[28] Roukos DH. Current status and future perspectives in gastric cancer management. Cancer Treat Rev 2000; 26: 243-255.

[29] Yasui W, Sentani K, Sakamoto N, Anami K, Naito Y and Oue N. Molecular pathology of gastric cancer: research and practice. Pathol Re Pract 2011; 207: 608-612.

[30] Zhang L, Cao Y, Wei M, Jiang X and Jia D. Long noncoding RNA-RNCR3 overexpression deleteriously affects the growth of glioblastoma cells through miR-185-5p/Krüppel-like factor 16 axis. J Cell Biochem 2018; 119: 9081-9089.

[31] Nandan MO, Yoon HS, Zhao W, Ouko LA, Chanchevalap S and Yang VW. Kruppel-like factor 5 mediates the transforming activity of oncogenic H-Ras. Oncogene 2004; 23: 3404-3413.

[32] Nandan MO, Chanchevalap S, Dalton WB and Yang VW. Kruppellike factor 5 promotes mitosis by activating the cyclin B1/Cdc2 complex during oncogenic Ras-mediated transformation. FEBS Lett 2005; 579: 4757-4762.

[33] Zhao J, Bian ZC, Yee K, Chen BP, Chien S and Guan JL. Identification of transcription factor KLF8 as a downstream target of focal adhesion kinase in its regulation of cyclin D1 and cell cycle progression. Mol Cell 2003; 11: 1503-1515.

[34] Fernandez-Zapico ME, Lomberk GA, Tsuji S, DeMars CJ, Bardsley MR, Lin YH, Almada LL, Han JJ, Mukhopadhyay D, Ordog T, Buttar NS and Urrutia R. A functional family-wide screening of SP/KLF proteins identifies a subset of suppressors of KRAS-mediated cell growth. Biochem J 2011; 435: 529-537.

[35] Vo K, Amarasinghe B, Washington K, Gonzalez A, Berlin J and Dang TP. Targeting notch pathway enhances rapamycin antitumor activity in pancreas cancers through PTEN phosphorylation. Mol Cancer 2011; 10: 138.

[36] Eliasz S, Liang S, Chen Y, De Marco MA, Machek O, Skucha S, Miele L and Bocchetta M. Notch-1 stimulates survival of lung adenocarcinoma cells during hypoxia by activating the IGF-1R pathway. Oncogene 2010; 29: 2488-2498.

[37] Tetreault MP, Yang Y and Katz JP. Krüppel-like factors in cancer. Nat Rev Cancer 2013; 13: 701-713.

[38] Li L, Tang P, Li S, Qin X, Yang H, Wu C and Liu Y. Notch signaling pathway networks in cancer metastasis: a new target for cancer therapy. Med Oncol 2017; 34: 180.

[39] Zhu Z, Yu Z, Wang J, Zhou L, Zhang J, Yao B, Dou J, Qiu Z and Huang C. Krüppel-like factor 4 inhibits pancreatic cancer epithelial-to-mesenchymal transition and metastasis by down-regulating caveolin-1 expression. Cell Physiol Biochem 2018; 46: 238-252.

[40] Wang X, Lu H, Urvalek AM, Li T, Yu L, Lamar J, DiPersio CM, Feustel PJ and Zhao J. KLF8 promotes human breast cancer cell invasion and metastasis by transcriptional activation of MMP9. Oncogene 2011; 30: 1901-1911.

[41] Wang X, Zheng M, Liu G, Xia W, McKeown-Longo PJ, Hung MC and Zhao J. Kruppel-like factor 8 induces epithelial to mesenchymal transition and epithelial cell invasion. Cancer Res 2007; 67: 7184-7193.

[42] Panarese I, De Vita F, Ronchi A, Romano M, Alfano R, Di Martino N, Zito Marino F, Ferraccio F and Franco R. Predictive biomarkers along gastric cancer pathogenetic pathways. Expert Rev Anticancer Ther 2017; 17: 417-425.

[43] Wang C, Li L, Duan Q, Wang Q and Chen J. Krüppel-like factor 2 suppresses human gastric tumorigenesis through inhibiting PTEN/AKT signaling. Oncotarget 2017; 8: 100358-100370.

[44] Mao A, Zhou X, Liu Y, Ding J, Miao A and Pan G. KLF8 is associated with poor prognosis and regulates glycolysis by targeting GLUT4 in gastric cancer. J Cell Mol Med 2019; 23: 5087-5097.

# Krüppel-like factor 16 is a prognostic biomarker for gastric cancer
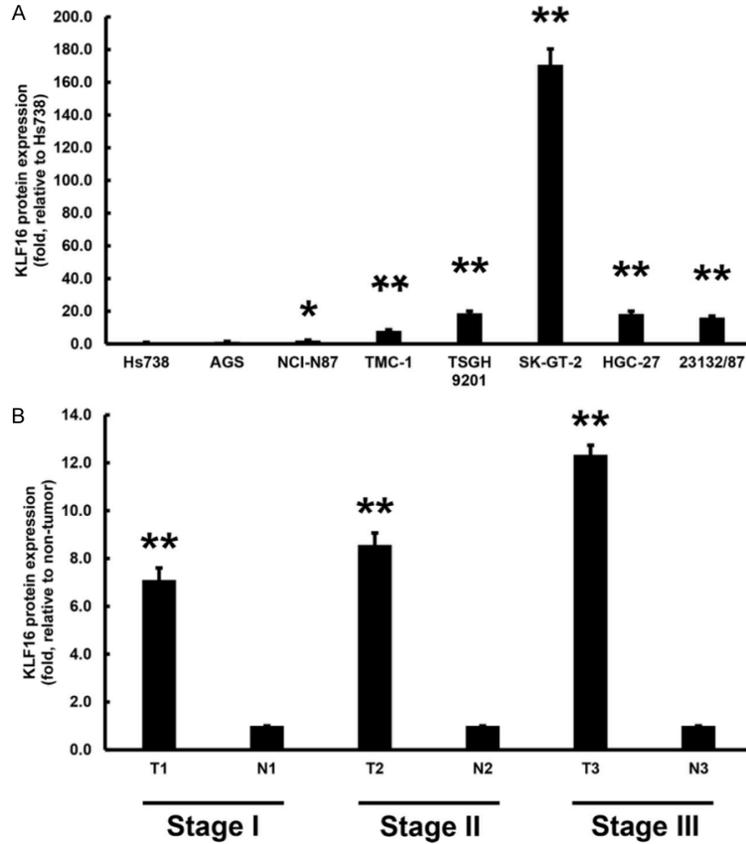
Figure S1. The quantification data of KLF16 protein expression in gastric cells and tissues. A. KLF16 protein levels were significantly increased in TMC-1, TSGH 9201, SK-GT-2, HGC-27 and 23132/87 cells. *denotes $P < 0.05$ compared with Hs738.St/Int cells; **denotes $P < 0.01$ compared with Hs738.St/Int cells. B. KLF16 protein levels were significantly increased in GC tissues. **denotes $P < 0.01$ compared with non-tumor tissues.
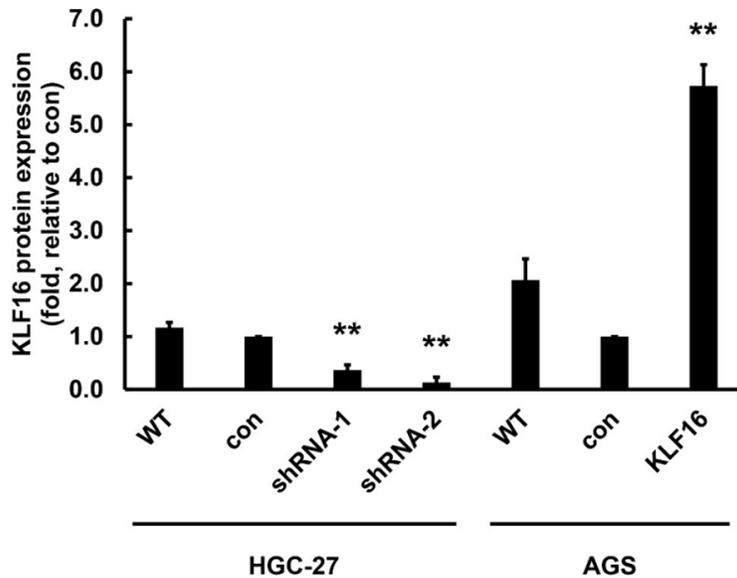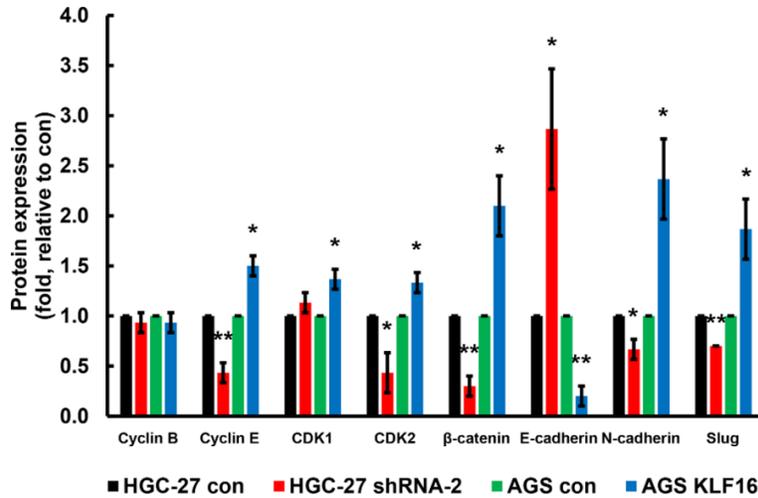

Figure S2. The quantification data of KLF16 protein expression in KLF16 knockdown and overexpressing GC cells. Stable KLF16 knockdown and overexpression significantly decreased and increased the expression of KLF16. **denotes $P < 0.01$ compared with the con cells. WT: non-transduced or non-transfected cells; con: scrambled control or control vector-transfected cells; shRNA: KLF16-knockdown cells; KLF16: KLF16-overexpressing cells.

Krüppel-like factor 16 is a prognostic biomarker for gastric cancer
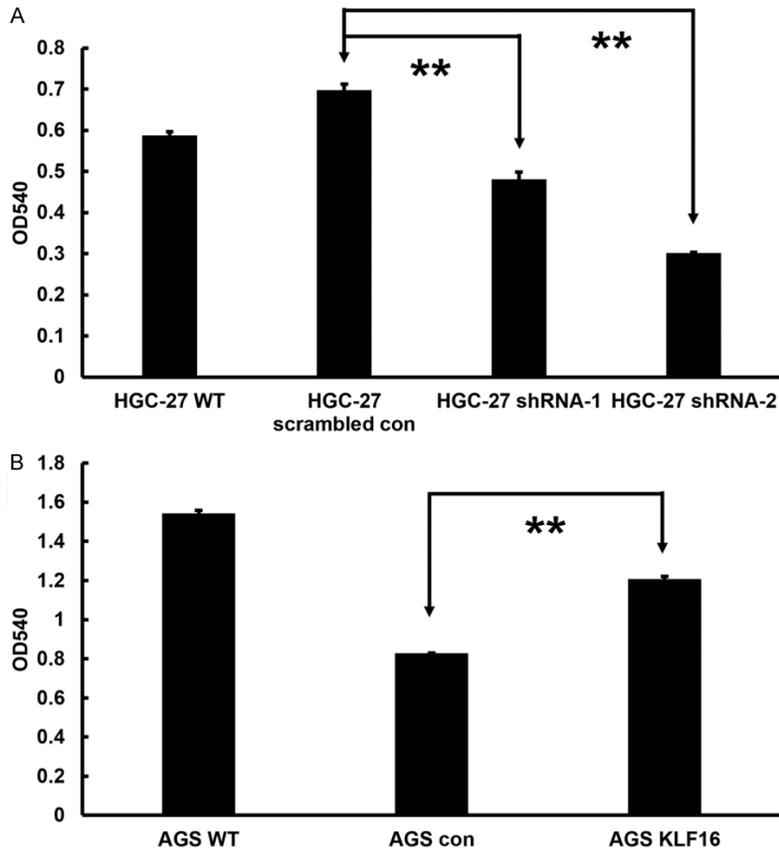
Figure S3. The quantification data of colony formation assay to show the effect of stable KLF16 manipulation on cell growth. A. Stable KLF16 knockdown results in significantly decreased OD540. The bar graph represents the OD540. **denotes *P* < 0.01 compared with the control. B. Stable KLF16 overexpression results in significantly increased OD540. **denotes *P* < 0.01 compared with the control. WT: non-transduced or non-transfected cells; con: scrambled control or control vector-transfected cells; shRNA: KLF16-knockdown cells; KLF16: KLF16-overexpressing cells.

Figure S4. The quantification data of cell cycle- and EMT-related protein expressions in KLF16 knockdown and overexpressing GC cells. Stable KLF16 knockdown significantly decreased the expressions of cyclin E, CDK2, β-catenin, N-cadherin and Slug and increased the expression of E-cadherin. Stable KLF16 overexpression significantly increased the expressions of cyclin E, CDK2, β-catenin, N-cadherin and Slug and decreased the expression of E-cadherin. *denotes *P* < 0.05 compared with the con cells; **denotes *P* < 0.01 compared with the con cells. con: scrambled control or control vector-transfected cells; shRNA: KLF16-knockdown cells; KLF16: KLF16-overexpressing cells.

2

Figure S5. The effect of stable KLF16 manipulation on PI3K and phospho-AKT levels in GC cells. Stable KLF16 knockdown and overexpression significantly decreased and increased the levels of PI3K and phospho-AKT, respectively. con: scrambled control or control vector-transfected cells; shRNA: KLF16-knockdown cells; KLF16: KLF16-overexpressing cells. *denotes $P < 0.05$ compared with the con cells; **denotes $P < 0.01$ compared with the con cells. con: scrambled control or control vector-transfected cells; shRNA: KLF16-knockdown cells; KLF16: KLF16-overexpressing cells.
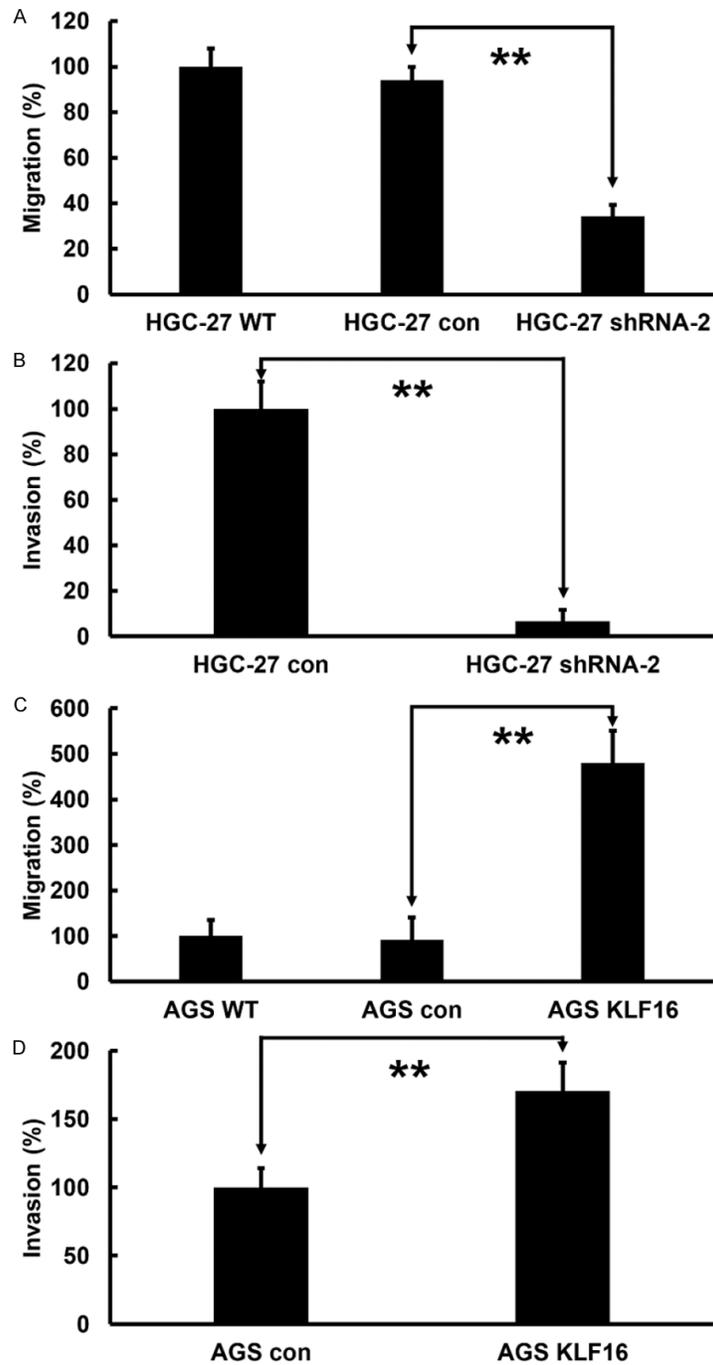
Figure S6. The quantification data of wound-healing and cell invasion assays to present the effect of stable KLF16 manipulation on cell spread. Stable KLF16 knockdown significantly decreased cell migration (A) and invasion (B). The bar graph represents the number of migrated and invaded cells relative to the control group (%, presented as the mean ± SD, **P < 0.01). Stable KLF16 overexpression significantly increased cell migration (C) and invasion (D). The bar graph represents the number of migrated and invaded cells relative to the control group (%, presented as the mean ± SD, **P < 0.01). WT: non-transduced or non-transfected cells; con: scrambled control or control vector-transfected cells; shRNA: KLF16-knockdown cells; KLF16: KLF16-overexpressing cells.
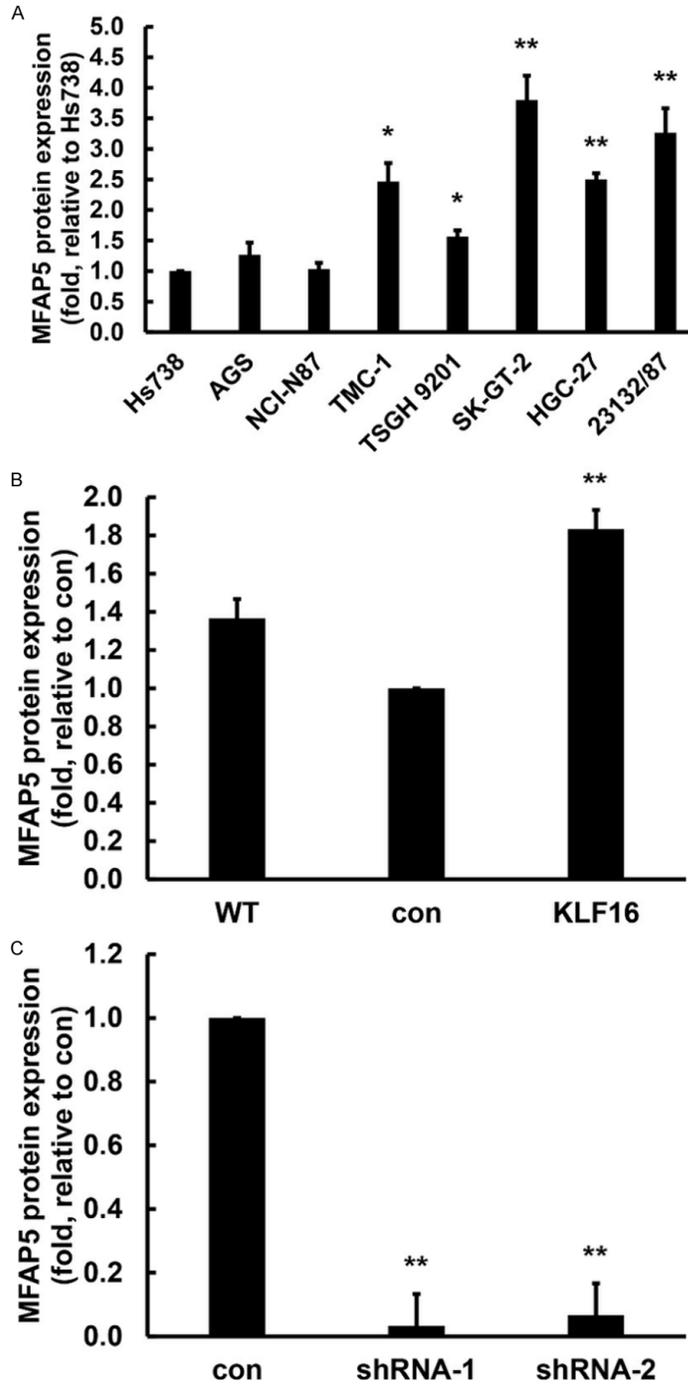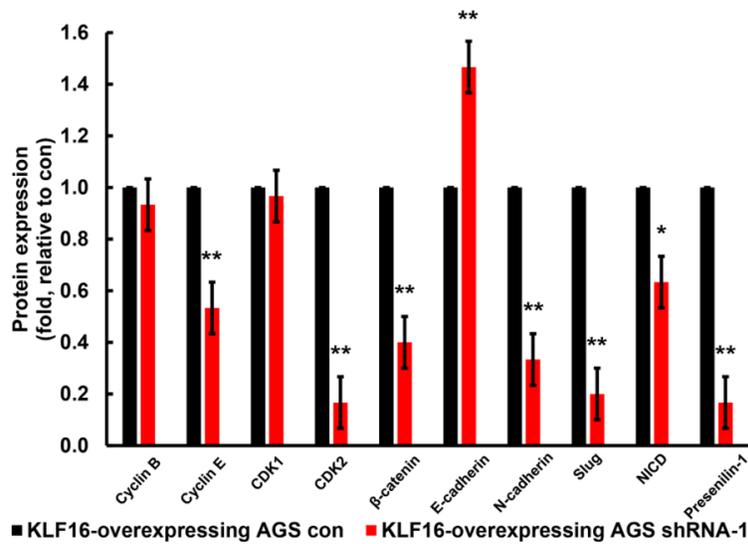
Figure S7. The quantification data of MFAP5 protein expression in gastric cells. A. KLF16 protein levels were significantly increased in TMC-1, TSGH 9201, SK-GT-2, HGC-27 and 23132/87 cells. *denotes $P < 0.05$ compared with Hs738.St/Int cells; **denotes $P < 0.01$ compared with Hs738.St/Int cells. B. Stable KLF16 overexpression significantly increased the expression of MFAP5 in AGS cells. **denotes $P < 0.01$ compared with the con cells. C. Stable MFAP5 knockdown significantly decreased the expression of MFAP5 in KLF16-overexpressing AGS cells. **denotes $P < 0.01$ compared with the con cells. WT: non-transfected cells; con: control vector-transfected or scrambled control cells; KLF16: KLF16-overexpressing cells; shRNA: MFAP5-knockdown cells.
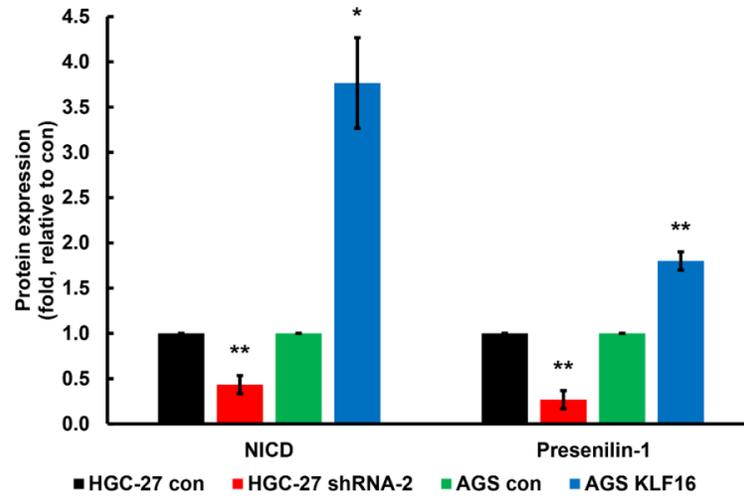
Figure S8. The quantification data of NICD and presenilin-1 protein expressions in KLF16 knockdown and overexpressing GC cells. Stable KLF16 knockdown and overexpression significantly decreased and increased the expressions of NICD and presenilin-1. *denotes *P* < 0.05 compared with the con cells; **denotes *P* < 0.01 compared with the con cells. con: scrambled control or control vector-transfected cells; shRNA: KLF16-knockdown cells; KLF16: KLF16-overexpressing cells.


Figure S9. The quantification data of cell cycle-, EMT- and Notch-related protein expressions in MFAP5-knockdown, KLF16-overexpressing AGS cells. Stable MFAP5 knockdown significantly decreased the expressions of cyclin E, CDK2, β-catenin, N-cadherin, Slug, NICD and presenilin-1 and increased the expression of E-cadherin. Stable MFAP5 overexpression significantly increased the expressions of cyclin E, CDK2, β-catenin, N-cadherin, Slug, NICD and presenilin-1 and decreased the expression of E-cadherin. *denotes *P* < 0.05 compared with the con cells; **denotes *P* < 0.01 compared with the con cells. con: scrambled control cells; shRNA: MFAP5-knockdown cells.
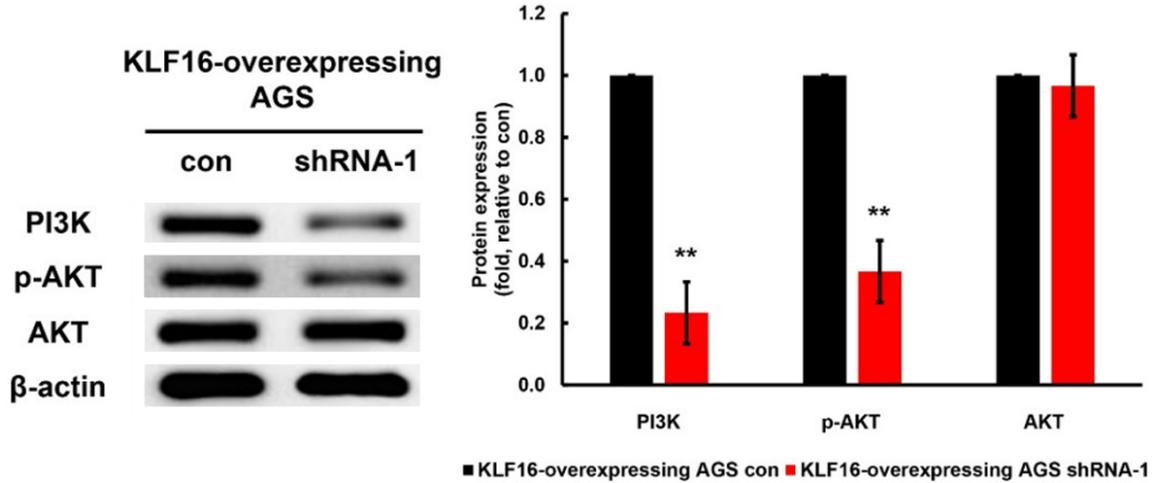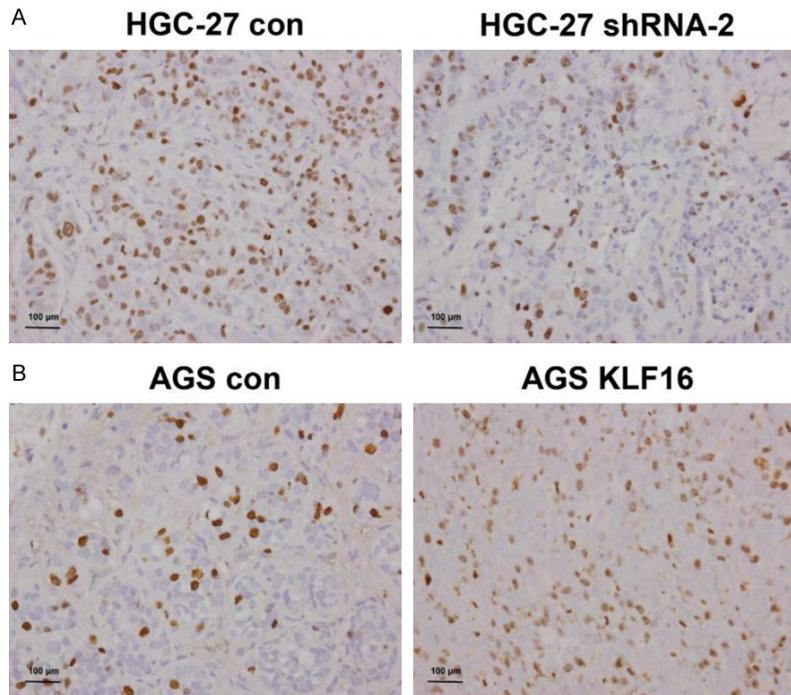
Figure S10. The effect of stable MFAP5 knockdown on PI3K and phospho-AKT levels in KLF16-overexpressing AGS cells. Stable MFAP4 knockdown markedly decreased the levels of PI3K and phospho-AKT. con: scrambled control cells; shRNA: MFAP5-knockdown cells. **denotes $P < 0.01$ compared with the con cells. con: scrambled control cells; shRNA: MFAP5-knockdown cells.
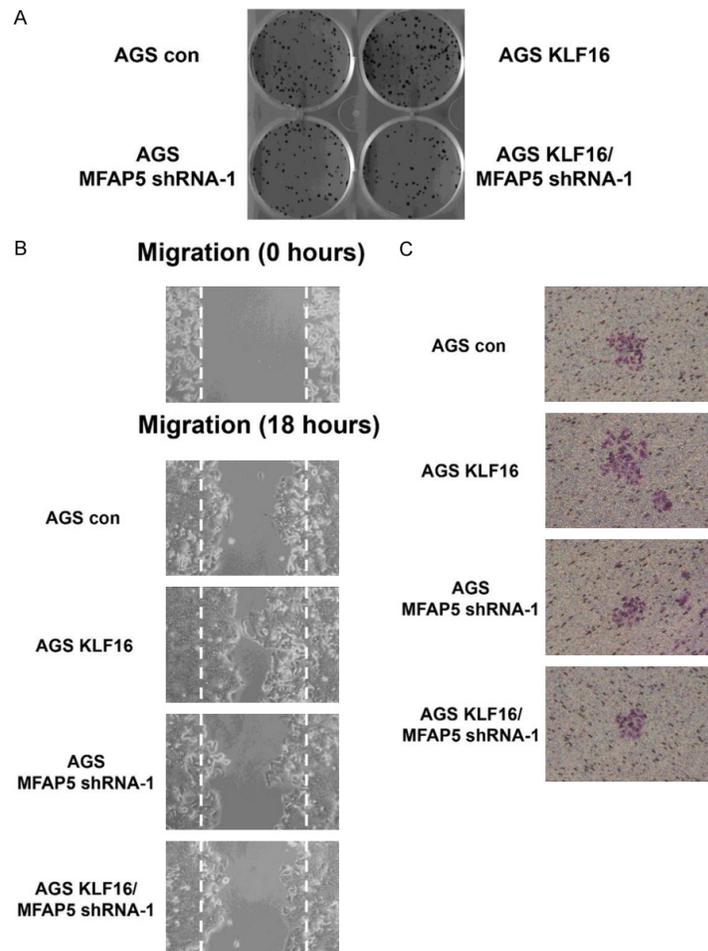
Figure S11. Effect of MFAP5 knockdown in control and KLF16-overexpressing AGS cells on cell growth and spreading. A. Stable MFAP5 knockdown obviously suppressed the cell proliferation of KLF16-overexpressing AGS cells, but not control AGS cells. B. Stable MFAP5 knockdown obviously suppressed the cell migration of KLF16-overexpressing AGS cells, but not control AGS cells. C. Stable MFAP5 knockdown obviously suppressed the cell invasion of KLF16-

overexpressing AGS cells, but not control AGS cells. WT: non-transduced cells; con: scrambled control cells; shRNA: MFAP5 knockdown cells. con: scrambled control or control vector-transfected cells; KLF16: KLF16-overexpressing cells.

Figure S12. The effect of stable KLF16 manipulation in HGC-27 and AGS cells on Ki67 expression in xenografts of nude mice. A. Stable KLF16 knockdown resulted in a significant decrease of Ki67 expression in xenografts, examined by immunohistochemistry. Magnification: 200×. B. Stable KLF16 overexpression resulted in a significant increase of Ki67 expression in xenografts, examined by immunohistochemistry. Magnification: 200×. con: scrambled control or control vector-transfected cells; shRNA: KLF16-knockdown cells; KLF16: KLF16-overexpressing cells.